Solid State Isotope Exchange with Spillover Hydrogen in Organic Compounds

Yu. A. Zolotarev,*,† A. K. Dadayan,† Yu. A. Borisov,‡ and V. S. Kozik†

Institute of Molecular Genetics, Russian Academy of Sciences, pl. Kurchatova 2, Moscow, 123182 Russia, and Nesmeyanov Institute of Organoelement Compounds, Russian Academy of Sciences, ul. Vavilova 28, Moscow, 119991 Russia

Received February 17, 2010

Contents

1. Background of the Spillover Hydrogen

The term spillover, as used in heterogeneous catalysis, refers to the transport of active particles which are either absorbed or formed in one phase and transported to another phase where, under these reaction conditions, such particles are not absorbed or formed. An example is that of hydrogen, which after dissociative adsorption on platinum particles can migrate onto a nonorganic support such as aluminum oxide, barium sulfate, or others. Such active hydrogen atoms were given the name spillover hydrogen (SH).[1] The first direct evidence of spillover was obtained during the reduction of wolfram trioxide to tungsten bronze at room temperature:[2] the reaction proceeds in a mechanical mixture of 0.5% Pt/Al_2O_3 + WO_3. It was assumed that the hydrogen dissociated on the platinum and migrated through the alumina onto WO_3 in the form of atoms or H^+ ions. The solid state hydrogenation of asymmetric crystals of 2-isopropyl-5-methylphenol (also known as thymol) occurs with the participation of SH and leads to the formation of a series of asymmetric menthols and menthones.[3]

Despite the fact that processes involving SH have been known for over 40 years, the nature of this phenomenon has not been fully investigated or clarified. According to various hypotheses, hydrogen can migrate in the form of a solvated proton,[4] as a proton−electron pair,[5] or as atomic hydrogen.[6] The main difficulty in explaining the SH phenomenon is that the SH concentration is too small to detect using direct instrumental analysis such as modern spectroscopic methods. Because the importance of SH in heterogeneous catalysis cannot be underestimated, the debate regarding the nature of the activated hydrogen particles and their diffusion is still ongoing.[1]

The formation of catalytic centers is known to take place as a result of the action of SH on initially inactive surfaces.[7] A description of these new catalytic centers is the major element in understanding the mechanism of SH-controlled reactions. Although the kinetic processes involved in SH reactions have been reported in numerous publications and some of them are listed here, the activity and selectivity of the catalytic systems formed differ greatly from system to system. This is probably associated with their production prehistory. Solid acidic catalysts play an important role both in petroleum refining and in the chemical industry. The catalytic properties of zeolites, heteropolyacids, and sulfurized metal oxides are in many respects determined by the structure and properties of their acidic centers.[8] After the addition of about 1% of a platinum group metal into the catalyst and its subsequent introduction into the gaseous hydrogen phase, significant modification of the acidic centers of the solid catalyst takes place. The catalytic selectivity abruptly changes, and the result is the formation of highly effective (95−99%) selective catalysts suitable for carbohydrate isomerization.[9] A number of studies report that new Brønsted acid centers arise under the action of SH, which can promote highly selective hydroisomerization and hydrocracking.[1,10,11]

In numerous publications, studies are reported where the mechanism of isomerization reactions on acidic centers is

Yurii A. Zolotarev is Professor of Bioorganic Chemistry; since 1989, he has been a Leading Researcher and Head of Research Group in Department of Chemistry of Biologically Active Compounds at the Institute of Molecular Genetics, Russian Academy of Sciences. He synthesized a number of unique polystyrene and polyacrylamide chiral sorbents, allowing the quantitative resolution of racemic amino acids into optic isomers to be performed for the first time. He has investigated solid state catalytic hydration and isotope exchange reactions with participation of spillover tritium and analyzed the phenomenon of isotopic equilibrium of gaseous tritium and hydrogen atoms in a molecule of solid organic compound. In 2000, he was awarded the State Scholarship "To Outstanding Research Persons of Russia". Prof. Zolotarev is a member of the International Isotope Society, and he was the scientific advisor for five Ph.D. students. The list of his publications bears over 150 titles, including 22 patents of Russia, USA, France, and Great Britain.

* To whom correspondence should be addressed. E-mail: zolya@img.ras.ru.
† Institute of Molecular Genetics.
‡ Nesmeyanov Institute of Organoelement Compounds.

10.1021/cr100053w
Published on Web 06/10/2010

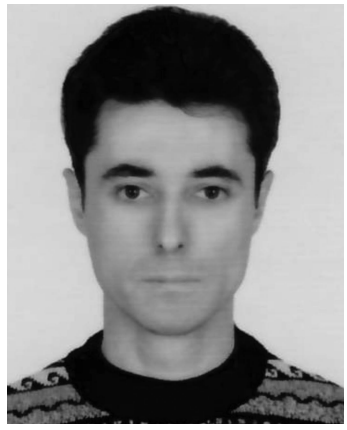

Alexander K. Dadayan received his first degree in chemistry at the M. V. Lomonosov Moscow State University in 1994. Since 1998, he has been a scientist at the Institute of Molecular Genetics Russian Academy of Sciences in Moscow. He received his Ph.D. in Physical Chemistry and Radiochemistry in 2004, working on examination of high temperature solid state isotope exchange of hydrogen for spillover tritium in peptides and proteins (under the direction of Prof. Yurii A. Zolotarev and Prof. Yurii A. Borisov). He has for the first time experimentally and theoretically analyzed the isotopic effect of electron excitation in [3H]Trp. His research interests include heterogeneous catalysis, isotope exchange with spillover hydrogen in organic compounds, and its usage in examination of the spatial structure of peptides and proteins, deuterium labeled organic compounds, and their application in quantitative mass spectrometry. He has published about 30 original studies.

Yurii A. Borisov is Professor of Physical Chemistry, Head of the Laboratory of Computational Chemistry at the A. N. Nesmeyanov Institute of Organoelement Compounds, Russian Academy of Sciences. He graduated from the Department of Chemistry, M. V. Lomonosov Moscow State University in 1963, and in 1971 received his Ph.D. in Chemistry from the Institute of Catalysis Siberian Branch of the USSR Academy of Sciences in Novosibirsk. In 1985 he received a Doctor of Science in Chemistry from the A. N. Nesmeyanov Institute of Organoelement Compounds, USSR Academy of Sciences. His research interests are in theoretical studies of the mechanisms of organic reactions that are of importance to environmental chemistry, studies of solvation effects on chemical reactions, and theoretical studies of the electronic structure and reactivity of organoelement and organometallic compounds. He has published about 300 papers and reviews in Russian and international scientific journals. Six Ph.D. theses were defended under his supervision.

studied using kinetic methods. As a result, several hypotheses on the different forms of activated hydrogen that appear in these reactions have been postulated. The isomerization reaction of *n*-butane on a $SO_4^{2-}-ZrO_2$ catalyst in the presence of Pt/SiO_2 has been shown to proceed on the acidic center in accordance with a monomolecular mechanism and did not lead to butene formation.[12] The reaction order is -1 at low temperatures and high hydrogen pressures, which is associated with the involvement of hydride in the catalysis.

Valerii S. Kozik is a Main Specialist of isotope technology at the Institute of Molecular Genetics, Russian Academy of Sciences in Moscow. He graduated from the Moscow D. Mendeleyev Institute of Chemical Technology. He first investigated reaction of solid phase catalytic hydration for preparing tritium labeled amino acids. He prepared the highly tritium labeled valine, which was used to analyze the mass of a neutrino. He organized the equipment for production isotope labeled physiologically active compounds at the Institute of Molecular Genetics, Russian Academy of Sciences. These labeled compounds are used in molecular biology, molecular genetics, and medicine.

The isomerization of *n*-pentane and the hydropyrolysis of cumene was studied using Pt/SiO_2 + zeolite H-beta and $Pt/SiO_2 + SO_4^{2-}-ZrO_2$ bifunctional catalysts.[13] The hydroisomerization reaction showed a positive order for hydrogen at low pressure: this is associated with an SH-affected increase in the catalytic power of the acidic centers. In the hydropyrolysis reaction, the effect of SH was more pronounced on sulfated zirconium oxide than on the H-beta zeolite. This is associated with a larger concentration of acidic centers on this catalyst. In another study,[14] the hydroisomerization of hexane and heptane on solid acids, for example cesium-containing Pt-ligated phosphorus tungstates, was studied. The catalyst showed a high selectivity (98% for hexane and 92% for heptane) at 180 °C. High conversion and stability to deactivation, which is believed to be due to the high stability of the acidic centers, were also observed.

The idea of the simultaneous formation of H^+ and H^- in SH underlies the interpretation of the experimental data on the bifunctional catalysis of hydrocarbon conversion.[15,16] Related investigations using the catalyst $Pt/SO_4^{2-}-ZrO_2$,- revealed that the action of SH leads to the conversion of the Lewis acidic centers to Brønsted acidic centers (BAC).[17,18] The strengthening of diphenyl methane cracking, observed after the addition of sulphidated $CoMo/SiO_2$ to the alumina silica catalyst, is associated with the formation of additional Brønsted acidic centers owing to the action of SH.[19]

The hypothesis that positively charged particles are formed during SH is supported by the fact that during SH a negative charge appears on the platinum group metal and the proton is transferred to the inorganic support.[20,21] In addition, SH-based processes are accelerated in the presence of H_2O.[10,22] The appearance of H^+ in SH on the zeolite surface agrees well with the model that describes SH particles as electron donors localized on the surface.[23] According to this model, an equilibrium between the charged (H^+) and atomic (H) forms of SH exists on the support. A kinetic model of bifunctional catalysis, based on these notions, has been proposed.[24] The electric properties of zeolites change under SH action. Additional positive charge-carrying particles are

formed, and these can be detected in the high-frequency resistance spectrum.[25] The dielectric relaxation process in the high-frequency area of the spectrum is associated with displacement of the protons arising under the effect of SH between adjacent Brønsted centers on the surface of the zeolites. The accelerating influence of water on SH is also explained by the fact that SH diffusion proceeds in the form of solvated protons. The fact that a homogeneous magnetic field directed perpendicularly to the direction of the spillover hydrogen decelerates its diffusion over the surface in two-component zeolite Pt/NaY-HNaY samples also supports the belief that SH is a charged particle.[26]

Proton migration over a surface bearing bound water and hydroxyl groups can proceed according to the relay mechanism with an activation energy of approximately 5 kcal/mol.[27] Surface-sorbed water molecules can participate in the SH transport, and the resulting acidic centers can enter the isotope exchange reaction. SH induces changes in the catalytic properties of the oxidized catalysts and the formation of new highly acidic Brønsted catalytic centers.[28] Under the action of SH, silica gel converts to an acidic catalyst that is capable of initiating reactions such as the hydrogenolysis and pyrolysis of benzene to acetylene. Such reactions are never observed in the absence of SH.[29] It was shown by spectroscopic methods that strongly acidic Brønsted-type centers in water-bound zeolites provide H_3O^+ ions hydrogen-bonded to the alumosilicate backbone.[30]

Deuterium exchange of the surface hydroxyl groups in Al_2O_3, SiO_2, and zeolites is widely used as a model reaction for studying the spillover deuterium, since this process can be easily monitored by IR spectroscopy. A correlation between the acidity of the OH and OD groups and the reactivity has been shown for H−D exchange in zeolites. This can be an indication of the ionic nature of SH.[31] In general, hydrogen exchange reactions for deuterium in organic compounds are conducted at very high temperatures (400−500 °C). Yet, if strongly acidic catalytic centers are involved, some reactions can proceed with sufficient rates at considerably lower temperatures. It appears that successive moderate temperature oxidation and reduction of the Pd/Al_2O_3 catalyst results in a sharp rise of its catalytic activity. Such a catalyst can be used to attain a considerable isotope reaction rate of hydrogen exchange for deuterium in cyclohexane at 25−55 °C.[32] Some kinetic studies showed that this considerable increase in the catalytic properties is linked with the formation of additional water molecules converted to new acidic catalytic centers under the action of SH on the catalyst surface. Catalysts obtained by conventional methods form no such acidic centers and are far less active in hydrogen isotope exchange reactions at temperatures below 200 °C.

Although there have been reports of a large number of selective catalytic reactions taking place on new acidic Brønsted centers formed under the effects of SH, it is only recently that the first theoretical quantum chemical study of the SH-affected conversion of catalytic centers has appeared. This is the basis for the "remote control" phenomenon.[33] In this review, we will summarize the available data on the study of the solid state reaction mechanism of SH involving organic compounds.

2. Main Regularities of Solid State Isotope Exchange Using Gaseous Deuterium and Tritium

High temperature solid state catalytic isotope exchange (HSCIE) reactions proceed under the action of deuterium or tritium at elevated temperatures in a solid mixture formed from an organic compound, an inorganic support, and a heterogeneous catalyst of platinum group metal (Figure 1).[34,35] Using this reaction, it becomes possible to substitute hydrogen for deuterium or tritium almost quantitatively in a series of amino acids. To date, the HSCIE reaction provides a unique experimental opportunity to produce such highly tritium-labeled compounds. The HSCIE reaction is also applicable to a range of organic compounds of different classes. A high degree of protium substitution for tritium in HSCIE is achieved when inert inorganic supports are pretreated with amino acids, biogenic amines, peptides, carbohydrates, nucleosides, or heterocyclic acids (Table 1).[36,37]

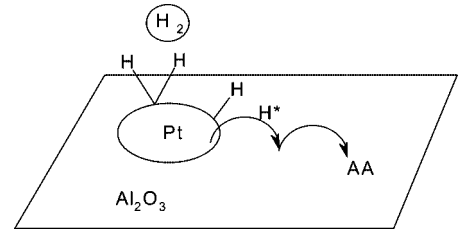

Figure 1. Schematic model of the HSCIE reaction between an amino acid (AA) applied onto an inorganic carrier (Al_2O_3) and spillover hydrogen (I*) activated on the catalyst.

Table 1. Tritium-Labeled Organic Compounds Synthesized Using HSCIE Reactions at 200 °C[a]

compound	specific activity, Ci/mmol	yield, %
L-alanine	65	90
L-phenylalanine	82	35
L-methionine	90	15
L-histidine	124	20
L-tryptophan	127	15
tryptamine	68	60
indolilacetic acid	82	32
stearic acid	811	14
hexadecylamine	850	9
biotin	43	12
adenosine	107	3

[a] Compounds are preliminarily deposited onto alumina and mixed with catalyst 5% Pd/$CaCO_3$. Redrawn from refs 36 and 37.

The spatial separation of the organic compound and the heterogeneous catalyst in a HSCIE reaction allows the introduction of the isotope label into different compounds, including those that are catalytic contaminators for the platinum metals. When compounds such as phenylalanine, histidine, indolyl acetic acid, tryptamine, or biotin are deposited on the catalyst, they completely decompose at 200 °C in a hydrogen atmosphere. With the HSCIE reaction, one can also obtain tritium-labeled compounds of high molar radioactivity at this low temperature.

An important specific feature of HSCIE reactions is that isotope exchange at 150−200 °C in amino acids and peptides proceeds with a high degree of retention of configuration of the carbon asymmetric atoms.[38,39] The virtually complete absence of racemization in HSCIE reactions makes this reaction a valuable preparative method. Ligand exchange chromatography was used for the analysis and preparative isolation of isotopically substituted amino acids.[40−42] Intensive isotope exchange between the gaseous phase hydrogen and the hydrogen atoms of the solid organic compound takes place at elevated temperatures in a solid mixture of a highly dispersed platinum group metal, a solid organic compound, and an inorganic support.

Table 2. Typical HSCIE Reaction Conditions for *O*-Methylserine with Tritium at Various Temperatures (5% $Pd/CaCO_3$ in the Presence of $PdCl_2$)[a]

	reaction temperature, °C			
parameter	135	150	170	200
avg tritium inclusion (atom)	0.31	0.83	2.34	4.41
tritium distribution in fragment (atom)				
H-Cα	0.11	0.23	0.53	0.75
H-Cβ	0.015	0.06	0.48	1.37
OMe	0.18	0.52	1.38	2.28
distribution of isotopomers in OMe, %				
CTH_2	70	51	46	15
CT_2H	26	39	41	42
CT_3	4	10	13	43
portion of amino acid in the reaction zone, %	25	40	100	100

[a] Redrawn from ref 48.

The phenomenon involving the isotopic equilibrium of gaseous hydrogen and the hydrogen atoms of the solid organic compound was first demonstrated using the HSCIE reaction.[34] In the isotopic equilibrium, the degree of substitution of the hydrogen atoms in an organic compound can only be determined using the total ratio of the protium and the isotope introduced by the reaction. Consecutive substitution of the gaseous reaction mixture for initial deuterium or tritium appears to be especially effective for increasing the isotopic substitution degree of the hydrogen in an organic compound. A HSCIE reaction with deuterium at 200 °C for 1 h was used to produce the D-labeled valine with 4.4 deuterium atoms (55% of the total C−H bonds). The substitution degree of hydrogen for deuterium was increased by up to 96%, with no change in the overall reaction time, in a 2-fold replacement of gaseous deuterium.[34]

An interesting fact about HSCIE reactions is that they proceed regioselectively in the 100−150 °C temperature range, leading to the formation of selectively labeled compounds. The correlation between the structure of the α-amino acids and their reactivity has been studied.[43,44] At temperatures of 180−200 °C and higher, isotope exchange at all H−C bonds proceeds evenly and leads to uniformly labeled compounds.[45]

The distribution analysis of isotopomers is an effective method in solid state reactions investigation. Data on the isotopomeric distribution in the methyl groups of amino acids and peptides make it possible to determine the ratio of isotopomers in the reaction zone at a chosen temperature. This particular analysis was carried out using tritium NMR spectrometry.[46] During the isotope equilibration for a given average degree of hydrogen substitution in the methyl group, an equiprobable distribution of the isotopomers CT_3, CT_2H, CTH_2, and CH_3 is observed. If only a part of the molecules in the solid phase is accessible for spillover tritium, more highly substituted isotopomers are formed. Table 2 shows the dependence of the average tritium content and distribution in L-[^{3}H]Ser(OMe) on the HSCIE reaction temperature.

Isotope exchange in amino acids is regioselective at temperatures of 135 °C and lower. Only a portion of the molecules appear to be accessible for participation in the reaction. The regioselectivity declines at temperatures of 180 °C and higher. Isotope exchange proceeds evenly in all H−C bonds with the formation of evenly labeled compounds. The extent of this substitution is determined solely by the ratio of hydrogen and other isotopic atoms in the system.[47,48] The distribution of tritium in the evenly tritium-labeled L-[^{3}H]Ser(OMe) with a molar radioactivity of 128 Ci/mmol was analyzed using ^{3}H NMR (Figure 2).[49]

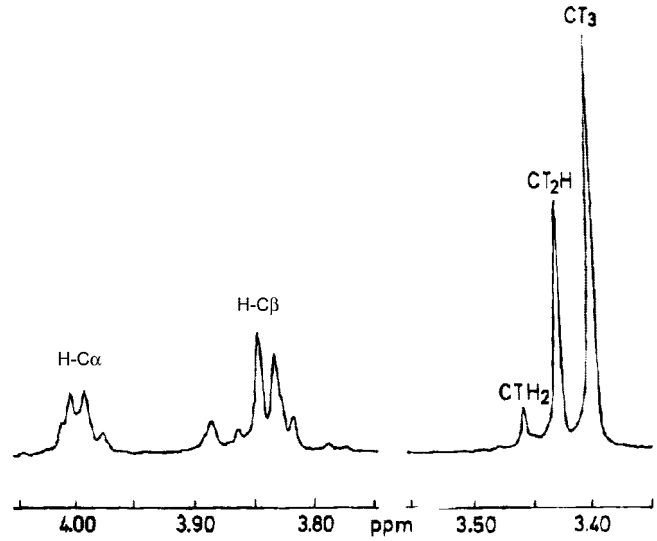

Figure 2. Proton-decoupled 266.8 MHz tritium spectra (in D_2O) of L-[^{3}H]Ser(OMe) (HSCIE at 200 °C, specific radioactivity 128 Ci/mmol). Redrawn from ref 48.

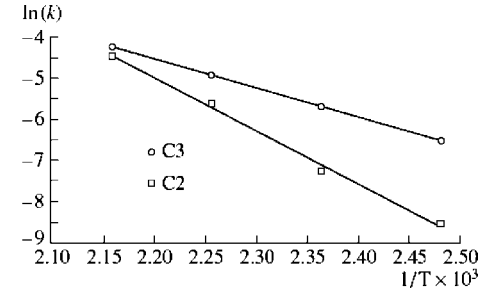

Figure 3. Dependence of ln(k) on T^{-1} for the HSCIE reaction of H-Cα (C2) and H-Cβ (C3) with tritium in L-alanine. Redrawn from ref 50.

The HSCIE activation energy for the different positions in a series of amino acids was calculated using the temperature dependence data of the rate of tritium−hydrogen exchange. The activation energy was found to be 14 and 25.7 kcal/mol for the methyl group and H-Cα in Ala, respectively.[50] Figure 3 shows the dependence of ln(k) on $1/T$ for the HSCIE reaction for hydrogen substitution at the carbon atoms Cα (C2) and Cβ (C3) in L-Ala for tritium.

The rate of H-Cβ exchange by tritium at 130 °C is 7.5 times higher than that of H-Cα. The isotope label selectively incorporates into the methyl group at 130 °C. At 190 °C, on the other hand, one can only speak of an even substitution of hydrogen for tritium into all the C−H bonds in the L-Ala molecule. It is well-known that the activation energy of a complex reaction is determined by its limiting step. It is also known that the limiting step of SH-involving reactions can be one of the following: the transition of the active hydrogen from the platinum metal surface or its migration over the inorganic surface or the reaction of SH with the applied substrate. The transition of active hydrogen from the platinum metal surface and its migration over the inorganic surface are the common steps for SH particles participating in the interaction with various positions of an alanine molecule. The fact that the isotope exchange reactions at different positions of the molecule proceed with different activation

Table 3. HSCIE Synthesis of Tritium-Labeled Tryptophan with Spatially Separated Substrate and Catalyst (Catalyst 5% Pd/$BaSO_4$, 25 kPa $^3H_2$)[a]

support	amino acid/ support ratio	temp, °C	degree of substitution	yield, %
$CaCO_3$	1:10	180	0.74	31
$CaCO_3$	1:20	180	1.26	27
$CaCO_3$	1:40	180	1.46	25
$CaCO_3$	1:80	180	3.38	20
$CaCO_3$	1:80	190	3.67	22
$CaCO_3$	1:80	200	4.47	15
$BaSO_4$	1:20	180	1.77	37
Al_2O_3	1:20	180	0.74	40

[a] Redrawn from ref 48.

energies indicates that the interaction of spillover tritium with the organic compound is the limiting step of the HSCIE reaction.

Many experiments have shown that the SH formed on the catalyst can migrate over the surface of the inorganic carrier and can enter into the exchange reaction with the surface O−H groups. The organic compound chosen for HSCIE is applied onto an inorganic support, and then a platinum group heterogeneous catalyst is introduced into the solid mixture. The isotope exchange reaction proceeds within the organic compound layer after the catalyst-activated SH diffuses into this layer. A wide range of inorganic salts and oxides are available to ensure hydrogen spillover from the catalyst into the organic compound to act as support in the HSCIE. The choice of inorganic support for each individual compound is made depending on its stability under HSCIE conditions as well as the reactivity of its C−H bonds. The effect of the temperature and the content of the solid state components on tritium incorporation into L-Trp are shown in Table 3.

The molar radioactivity grows with the increase in the reaction temperature, but there is a concomitant decrease in chemical yield. The chemical yield also decreases with the growth of the amino acid/support ratio. Optimization of the reaction conditions involves judicious choice of the support, the reaction temperature, and the compound/support ratio. In the case of L-Trp, a molar radioactivity of 97 Ci/mmol was produced for L-[^{3}H]Trp, at an amino acid/$CaCO_3$ ratio of 1:80 and a reaction temperature of 180 °C. Using ^{3}H NMR, it was shown that the tritium label was incorporated into all the amino acid C−H bonds. Under the same HSCIE conditions, with the exception of a smaller L-Trp/$CaCO_3$ ratio of 1:20, L-[^{3}H]Trp was produced with a molar radioactivity of 38 Ci/mol, while the isotope label distribution remained unchanged. These results indicate that the accessibility of amino acids for SH and the degree of hydrogen substitution for tritium or deuterium can be raised by increasing the inorganic support/organic compound ratio.[48]

The inorganic support plays not only the role of SH transporter but can also change the reactivity of the organic compounds being applied. HSCIE reactions with tritium and phenylalanine applied onto different supports showed that the distribution of the isotope label in the aromatic part of the molecule was the same when activated carbon, barium sulfate, and alumina oxide were employed as supports. Although the tritium distribution in the aliphatic part of the molecule is similar for activated carbon and barium sulfate in the reaction with alumina oxide as the support, hydrogen substitution increases at Cα from 10% to 40%. As shown by quantum-chemical modeling of this reaction, this increase in reactivity of hydrogen substitution at Cα can be attributed to the interaction of the amino acid carboxyl group with the alumina oxide.[51]

Table 4. Distribution of Tritium and Its Average Inclusion in Amino Acids for the HSCIE Reaction at 150 °C for 40 min[a]

amino acid	avg tritium inclusion (atom)	tritium distribution between the amino acid atoms, %				
		Cα	Cβ	Cγ	Cδ	Cε
Ala	0.45	4	96			
Asn	0.66	40	60			
Asp	0.21	40	60			
Arg	2.17	19	23	14	44	
Gly	0.21	100				
Hyp	0.52	6	7	5	83	
Pro	0.55	9	6	4	81	
Met	0.17	75		4	21	
Met(O)	0.34	14		25	61	
Met(O_2)	0.48			40	60	
Ser	0.52	70	30			
Ser(OMe)	0.72	29	7	64		
Thr	0.66	18	9	73		
Leu	0.90	4	5	5	86	
Ile	0.83	4	5	5	86	
Lys	1.76	31	10	12	18	29
Val	0.86	4	4	92		

[a] Redrawn from ref 44.

It has also been found that the exchange ability of the hydrogen atoms in HSCIE reactions can differ considerably from the corresponding ability in liquid state isotope exchange reactions. The activation energy of hydrogen isotope exchange is different for the different C−H bonds of solid organic compounds. The regioselectivity of HSCIE reactions for amino acids with spillover tritium was evaluated according to the tritium distribution in the labeled compound. Table 4 shows the results of the experimental study of HSCIE selectivity and the reactivity of a series of aliphatic acids at 150 °C.[44]

It was found that isotopic exchange in the aliphatic acids with no additional functional groups, such as Ala, Val, Leu, and Ile, preferentially proceeded in the methyl groups. The hydrogen atoms of the methyl groups in these amino acids have similar reactivities. Hydrogen atoms at the secondary and tertiary carbon atoms exhibit significantly lower reactivity in HSCIE. The reactivity of H-Cα rises considerably in amino acids such as Ser, Thr, Asp, and Asn. The relative reactivity of aspartic acid is lower, but that of the basic amino acids lysine and arginine is higher than that of aliphatic acids bearing no additional functional groups. The regioselectivity of these reactions will be discussed in more detail below using quantum-chemical modeling. An analysis of the substitution in aromatic amino acids made it possible to elucidate some important features of the HSCIE reaction (Table 5).

As much as 76% of the label in His is incorporated into its imidazole group. The side chain H-Cβ in Phe, Tyr, and Trp all display a high ability to exchange. Hydrogen substitution in Tyr is more active at C3 and C5 when in the *ortho*-positions with respect to the hydroxyl group. As quantum-chemical calculations show, this position carries the largest negative charge of the carbon atoms and, hence, shows the largest affinity for the proton: C3, 140 kcal/mol; C2, 132 kcal/mol.[44] The observed reactivity is in agreement with the electrophilic character of SH in HSCIE.[48] H-C2 shows the greatest propensity toward SH in the heteroaromatic group of Trp. In 5-hydroxytryptamine, hydrogen is more easily exchanged with position 4 of the indole fragment

Table 5. Distribution of Isotope Label in Aromatic Amino Acids and 5-Hydroxytryptamine after HSCIE Reaction at 150 °C for 40 min[a]

amino acid	average tritium inclusion (atom)	distribution of tritium in amino acids, %							
		Cα	Cβ	C2	C3	C4	C5	C6	C7
His	0.95	20	4	55			21		
Phe	0.66	13	40	4.5	16	6	16	4.5	
Tyr	0.62	11	35	6	21		21	6	
Trp	0.83	11	24	25		5	10	10	6
5-hydroxytryptamine	1.03	35	7	10		35		6	7

[a] Redrawn from ref 44.

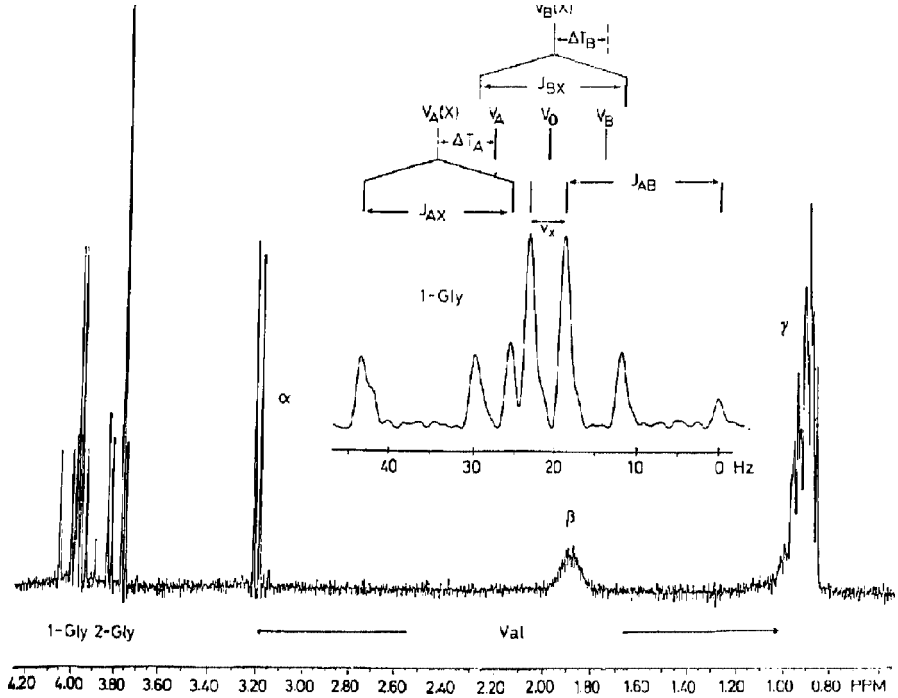

Figure 4. Tritium NMR spectra (266.8 MHz, without suppression of spin−spin interaction) of the peptide [U-^{3}H]Val-Gly-Gly (VGG) (HSCIE at 180 °C, specific radioactivity 208 Ci/mmol). Redrawn from ref 49.

in the *ortho*-position with respect to the hydroxyl group at C5. It is worth mentioning that the reactivity of H at C6, also in the *ortho*-position to this hydroxyl, is approximately 6 times smaller than that of H-C4. Such differences in reactivities are due to some specific features of the electronic structure of 5-hydroxytryptamine.

The isotope exchange reaction is a significant contributor to isotope label distribution in the solid phase hydration of multiple bonds in the unsaturated precursors of amino acids at temperatures between 80 and 120 °C.[52,53] The common feature of these reactions is that a larger amount of the stoichiometric tritium can be introduced into the amino acids, due to exchange at the allylic positions. Tritium incorporation increases considerably together with the temperature increase. Solid state hydration results in a greater yield of labeled amino acids than that resulting from traditional liquid phase hydration. Production of initial tritium-labeled unsaturated compounds alongside the saturated tritium-labeled compounds is possible under the reaction conditions for solid state hydration. Solid state hydration of 3,3-dimethyl-2-benzoylaminoacrylic acid resulted in the production of both labeled *N*-benzoylvaline and [Me-^{3}H]-3,3-dimethyl-2-benzoylaminoacrylic acid with a molar radioactivity of 8 Ci/mmol: all the isotope label was found in the methyl groups.[54] On the other hand, the catalyst-activated hydrogen enters the hydration reaction much more rapidly compared with the case of the isotope exchange reaction: no label introduction into the initial compound was observed. Solid phase hydration can proceed stereoselectively under the action of an asymmetric center in the initial compound. Solid state hydration of (*R*-4-*tert*-butoxy)-1,2-pyrroline-2-carboxylic acid applied onto a Pd/$BaSO_4$ catalyst resulted in the production of tritium-labeled *R*-4-*tert*-butoxyproline with a 6-fold excess of the L-form.[55]

HSCIE regioselectivity was also studied in peptides and proteins. The effect of the peptide structure on the reactivity of its C−H bonds was studied in a series of Gly-containing peptides GGV, GVG, VGG, GGH, GHG, and HGG.[48,49] At 150 °C, these amino acids demonstrated their greatest reaction ability when located at the N-terminal of the peptide chain. All the Gly fragments located in the middle portion of this series of tripeptides displayed practically the same degree of hydrogen substitution for tritium. Isotopomer distribution analysis of the Gly fragments showed that all the molecule constituents of the peptides are accessible for SH under the HSCIE reaction conditions. Hydrogen isotope exchange at 150 °C takes place at the most active positions of amino acid fragments, while the molar radioactivity of the labeled peptides depends on their initial structure. At 180 °C, a VGG peptide with a molar radioactivity of 208 Ci/mmol was obtained. This was the first reported instance of a labeled peptide with an even substitution of tritium (Figure 4). The total substitution of tritium for hydrogen reached about 70%, with racemization of the asymmetrical C_α in the

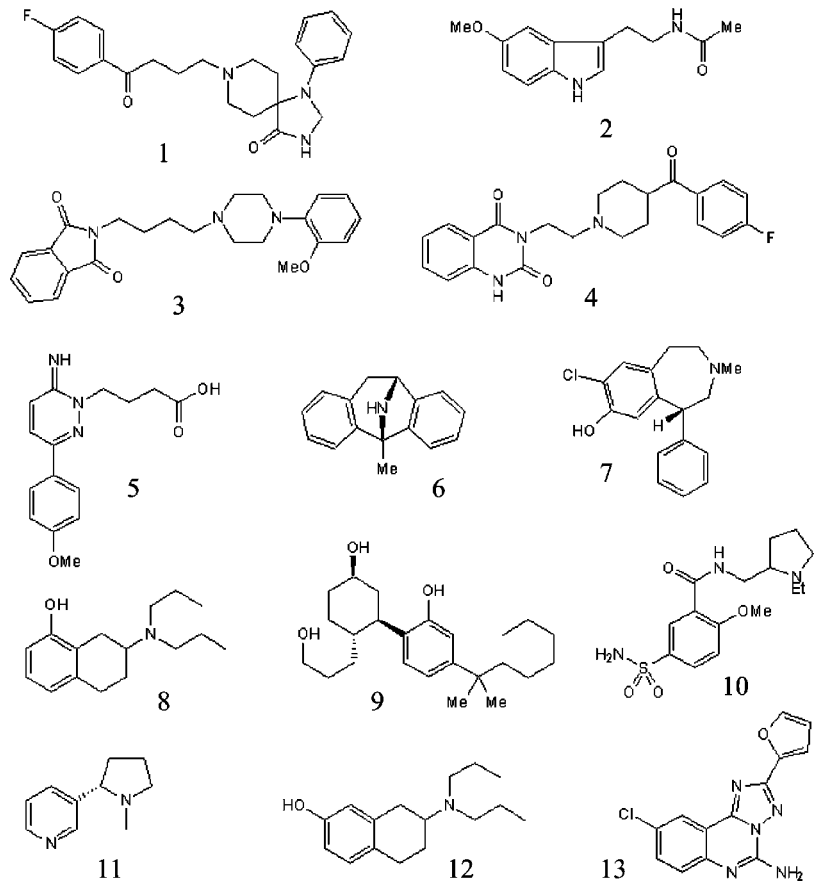

Figure 5. Tritium labeled selective ligands (HSCIE at 160−190 °C): **1**, [^{3}H]Spiperon (110 Ci/mmol); **2**, [^{3}H]Melatonin(140 Ci/mmol); **3**, [^{3}H]NAN-190(150 Ci/mmol); **4**, [^{3}H]Ketanserin (60 Ci/mmol); **5**, [^{3}H]SR95531 (120 Ci/mmol); **6**, [^{3}H]MK-801 (210 Ci/mmol); **7**, [^{3}H]SCH 23390 (60 Ci/mmol); **8**, 8-hydroxy-[^{3}H]DPAT (120 Ci/mmol); **9**, [^{3}H]CP 55940 (70 Ci/mmol); **10**, [^{3}H]Sulpiride (70 Ci/mmol); **11**, (−)[^{3}H]Nicotine (140 Ci/mmol); **12**, 7-Hydroxy-[^{3}H]DPAT (120 Ci/mmol); **13**, [^{3}H]CGS 15943(80 Ci/mmol). Redrawn from ref 58.

valine molecule not exceeding 1%. No racemization of amino acid fragments was observed in the solid state hydrogen exchange in the Arg-Arg-Ala-Ser-Val-Ala heptapeptide.[56]

The HSCIE reaction has been used in the production of highly tritium-labeled organic compounds of different classes. Tritium- and deuterium-labeled ligands of the glutamate and dopamine receptors were produced using this reaction.[57,58] Tritium-labeled (5*S*,10*R*)-(+)-5-methyl-10,11-dihydro-5H-dibenzo[*a*,*d*]cyclopenten-5,1-imine ([G-^{3}H]-MK-801) and *R*(+)-7-hydroxy-*N*,*N*-di-*n*-propyl-2-aminotetraline ([G-3H]-7-OH-DPAT) were obtained with a specific activity of 210 and 120 Ci/mol, respectively (Figure 5). It is noteworthy that the commercially available [3-^{3}H]-MK-801 has a molar radioactivity, 20 Ci/mmol, an order of magnitude smaller.[59] The average incorporation of deuterium into the uniformly deuterium-labeled [G-^{2}H](+)-MK-801 and [G-^{2}H]*R*(+)-7-OH-DPAT equals 11.09 and 3.21 atoms, respectively. Under electrospray conditions, a positive monovalent molecular ion of 222 Da was formed from MK-801. The distribution of isotopomers in [G-^{2}H](+)-MK-801 is shown in Figure 6 and Table 6. Neither unreacted starting compounds or deuterated molecules up to [$^2H_6$]-MK-801 were detected. The mean calculated rate of hydrogen substitution for deuterium was 11.09 deuterium atoms per molecule (79% of exhaustive substitution). Isotopomers [$^2H_{11}$]-MK-801 and [$^2H_{12}$]-MK-801 constitute about 69% of the total number of labeled molecules. The isotope label was shown to be distributed throughout the ligand molecule.

The radio-receptor binding of the tritium labeled [G-^{3}H](+)-MK-801 and [G-^{3}H]*R*(+)-7-OH-DPAT with the brain structures of Vistar rats was analyzed. It was found that [G-^{3}H]-MK-801 was specifically bound to the rat hippocampus membranes with $K_d = 8.3 \pm 1.4$ nM and $B_{max} = 3345 \pm 300$ fmol/mg of protein in this case. It was demonstrated that [G-^{3}H]*R*(+)-7-OH-DPAT bound specifically with the rat striatum membranes with $K_d = 10.01 \pm 0.91$ nM, with B_{max} in this case equal to 125 ± 4.5 fmol/mg protein. The ligand−receptor interaction parameters of the uniformly tritium-labeled ligands were in agreement with the literature data for selectively labeled ligands. Thus, it was clearly

Table 6. Mass-Spectrometric Analysis of Isotopomer Distribution in Deuterium-Labeled [G-^{2}H]-MK-801[a]

ion mass, Da	ion intensity, relative units	N_D	%
222	0	0	0.0
223	0	1	0.0
224	0	2	0.0
225	0	3	0.0
226	0	4	0.0
227	0	5	0.0
228	0	6	0.0
229	58047	7	0.2
230	257939	8	0.7
231	1895976	9	5.1
232	7654843	10	20.5
233	13786189	11	35.6
234	12856783	12	33.2
235	3331904	13	5.1
236	175000	14	0.3

[a] Number (N_D) and content (%) of deuterium atoms in the isotopomer. Average substitution degree: 11.09 ^{2}H per molecule (79.2%). Redrawn from ref 57.

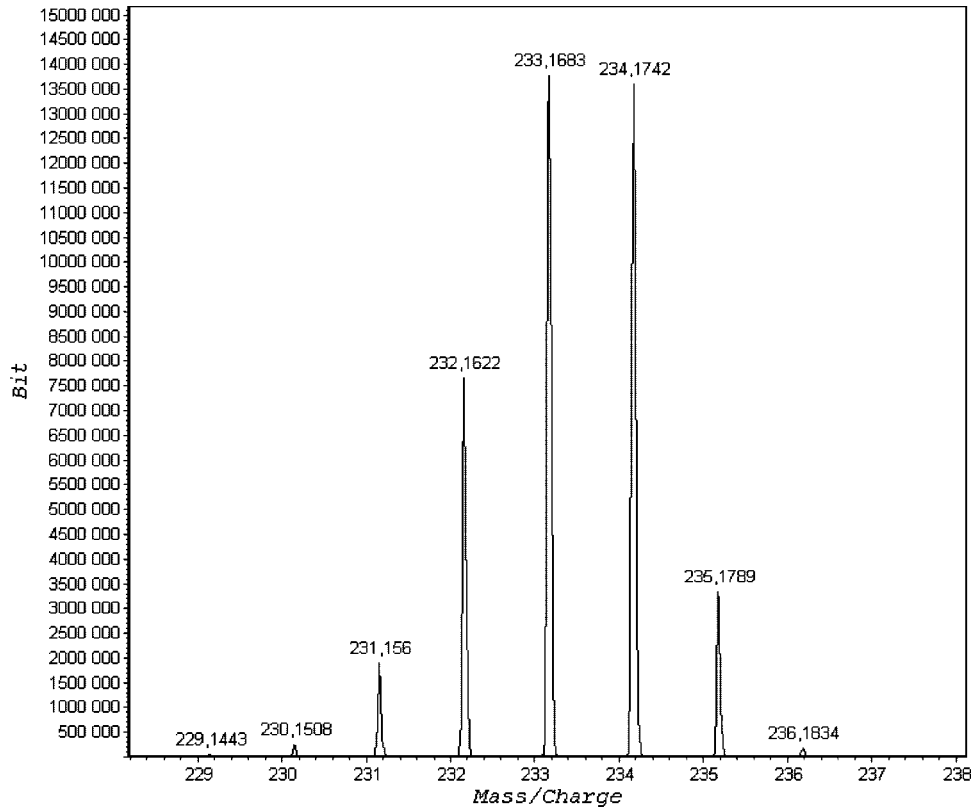

Figure 6. Section of [G-^{2}H](+)-MK-801 mass spectra. Redrawn from ref 57.

shown that the HSCIE reaction can be successfully employed for the production of highly tritium-labeled ligands while retaining their physiological activity.

3. Theoretical Investigation of the HSCIE Reaction

The theoretical study of the solid state isotope exchange reaction was instigated after the experimental investigation of the regioselectivity and the activation energies of tritium for protium substitution at various positions in amino acids. The results of the HSCIE reaction in amino acids at 150 °C are shown in Tables 4 and 7. For Ala and Val molecules, the first atoms to be substituted by tritium are the primary hydrogen atoms of the methyl groups because the hydrogen atoms bound with the secondary and tertiary carbon atoms are considerably less prone to exchange. This type of ratio between reactivities of C−H bonds of amino acids is somewhat uncommon, since usually the most mobile hydrogen atom at Cα is the first one to be involved in the majority of liquid phase reactions. The first step in understanding the HSCIE reaction mechanism was enabled by quantum and chemical modeling of the interaction of amino acids with activated hydrogen of various origins. At the beginning of the investigation, there was no unambiguous information in the literature as to the nature of the activated hydrogen participating in solid state isotope exchange reactions. It is well-known that, in the solid phase, hydrogen atoms in amino acids can be substituted by isotopic atoms under the action of thermally atomized tritium.[60,61] This method has been successfully used for studying the three-dimensional interaction of proteins within protein−protein complexes and in viral particles.[62,63] In this case, tritium reacts as a radical particle, resulting in the intermediate formation of an amino acid radical. The substitution ability of hydrogen in the amino acid in this case corresponds to the stability of the amino acid radical formed. The easiest substitution under the action of atomized tritium is the one that proceeds at the tertiary carbon atoms. The methyl groups of alanine, leucine, isoleucine, and valine appear to be the least reactive.[64] In this case, the substitution under the action of atomized tritium is accompanied by major racemization of the asymmetric atoms.[65] If tritium spillover reacted as a radical particle in HSCIE, then the reactivity of the methyl group of alanine and valine would also be expected to be lower than that of the other positions.

Table 7. Proton Affinities (PA, kcal/mol) of Aliphatic Amino Acids and Distribution of Effective Charges (*q*/e in the Units of Electron Charge) on the Atoms of These Amino Acids (According to Mulliken) Obtained from the AM1 Calculations[a]

	Cα		Cβ		Cγ		Cδ	
amino acid	PA	*q*/e	PA	*q*/e	PA	*q*/e	PA	*q*/e
Ala	83.0	−0.06	88.5	−0.23				
Val	87.9	−0.01	90.9	−0.10	99.9	−0.22		
Ser	74.5	−0.05	80.8	−0.01				
Thr	80.8	0.07	82.2	0.01	93.5	−0.26		
Pro	78.1	−0.07	85.5	−0.17	77.7	−0.17	88.6	−0.08

[a] Redrawn from ref 44.

The order of reactivity of organic compounds can radically change with any changes in the isotope exchange reaction mechanism. In the case of tritium thermal atomization, the hydrogen substitution in Phe proceeds exclusively in the side chain.[66] On the other hand, during acid homogeneous catalysis, it occurs almost always in the aromatic nuclei.[67] When isotope exchange between Phe and gaseous tritium takes place on heterogeneous platinum catalysts in solution, the isotope substitution involves the H-Cβ of Phe with high selectivity.[68] The experimental data available on the regioselectivity of HSCIE reactions in amino acids (Table 4 and

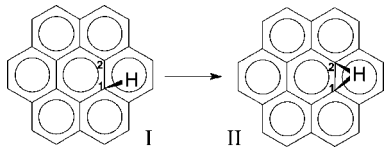

Figure 7. Complex of the modeled coronene complex $C_{24}H_{13}^+$ with a proton and transition state of proton transport. Redrawn from ref 69.

5) as well as the fact that hydrogen isotope exchange at asymmetric Cα atoms proceeds with configuration retention leads safely to the assumption that the activated tritium in HSCIE does not react like an atomized particle.

The first step in understanding the reaction mechanism of solid state catalytic isotope exchange involved analyzing the correlation between the electronic structure and the reactivity in HSCIE reactions of the free amino acid molecules. Quantum-chemical calculations of the geometric and electronic structure of α-amino acids were performed. The resulting charge distributions in the amino acids are presented in Table 7. The C-atoms of the alanine and valine methyl groups bear the largest negative charges, and according to the experimental data, the hydrogen atoms of these groups are in fact the ones predominantly exchanged by tritium. The same pattern has been observed for the threonine reaction. These amino acids show a common trend: the higher the negative charge on the C-atom, the easier the exchange of the bonded hydrogen atoms.[44] Thus, the correlation of the calculated charges of C atoms with the reactivity of the bonded H atoms supports the electrophilic nature of SH as it occurs in the HSCIE reaction. This correlation is not observed if the carbon in the amino acid is immediately connected to a negatively charged N or O atom. As has been shown in the case of proline, methionine, as well as some other amino acids, the preferential substitution of tritium for hydrogen proceeds in those carbons that are not carrying a considerable negative charge. The results of this *ab initio* study of SH and amino acid interactions helped to explain the deviation from simple correlations between the charges on the C atoms and reactivity in HSCIE reactions.

Quantum-chemical modeling of SH on a graphite-like surface was carried out in order to facilitate selection of the most likely hypothesis regarding the nature of SH migrating over an inorganic support.[69] Hartree−Fock (HF/6-31G*) *ab initio* calculations were performed not only for the model coronene ($C_{24}H_{12}$) complex which has a plane graphite-type frame but also for one of its complexes with the proton as well as the migration transition state of the proton on the model surface (Figure 7). Structure I corresponds to the proton located on the model graphite surface, and structure II to the transition state during the migration of a proton from one carbon atom to another. This models the spillover hydrogen process on the graphite support. The proton located on the model graphite support (structure I) is found on top of one of the surface atoms. In the transition state, the distances from the proton to the adjacent carbon atoms are equal, and the proton itself is on a line that is perpendicular to the surface plane and passes through the middle of the C_1-C_2 bond. The affinity to protonate was calculated to be 186.03 kcal/mol for $C_{24}H_{12}$, and the activation energy of the proton transfer between adjacent atoms was 10.0 kcal/mol. This corresponds rather closely to the experimentally determined value of 15.5 kcal/mol for the E_{act} of SH on a graphite surface.[70] The interaction of hydrogen in the form of a radical particle with C1 is thermodynamically disadvantageous,

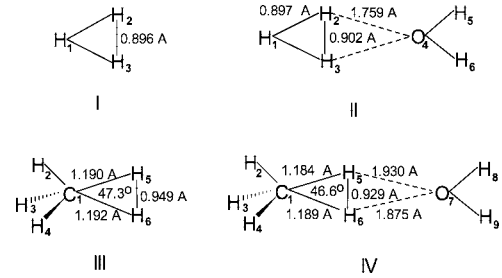

Figure 8. Structures of complexes with a proton H_3^+ (I) and CH_5^+ (III) and transition states of the reaction of hydrogen exchange between the H_3O^+ ion and H_2 (II) and CH_4 (IV) molecules (MP2/6-31G*). Redrawn from ref 75.

because the enthalpy of such a reaction is only 36.3 kcal/mol.[69] The data from such quantum-modeling of spillover hydrogen on a graphite-like surface supports the hypothesis that SH migrates over the inorganic surface as a positively charged particle. This hypothesis is also supported by earlier experimental evidence that demonstrated both electronic and ionic conductivity from the study of hydrogen spillover on a graphite surface.[71] No EPR signal from the atomic hydrogen was detected during SH.[72] Hydrogen spillover is accompanied by the emergence of a negative charge on the platinum group metal and by proton transfer onto the inorganic support. This leads to the formation of conductivity in the surface layer and to the emergence of semiconductive properties.[32] The presence of positively charged particles on the zeolite surface is detected in the high frequency resistance spectrum.[37]

Quantum-chemical calculations of proton interactions with amino acids in HSCIE reactions as well as for the energies of formation of amino acid−proton complexes were determined. In these complexes, a proton binds to the saturated carbon atom to form a structure with a pentacoordinated carbon atom. The basis for these calculations was the structure, in the gas phase, of the methonium ion CH_5^{+}.[73] The methonium ion structure, shown in Figure 8, was calculated according to the Hartree−Fock methods (HF/6-31G*) and MP2/6-31G*.[74,75]

The electronegative nitrogen and oxygen atoms of the NH_2, COOH, and OH groups were shown to exhibit the largest proton affinities.[76] This agrees well with the fact that the hydrogen found at these positions is easily replaced by tritium in HSCIE reaction even at room temperature. Isotope exchange at the C−H bonds, on the other hand, only reaches considerable rates at temperatures higher than 100 °C. Since the isotope label easily washes out from these labile positions during the subsequent interaction of the solid phase with the solvent during the isolation process for the labeled amino acid, it is therefore necessary to establish the correlations between the isotope exchange regioselectivity at the C−H bonds and the affinity of the different positions of amino acids to protonate. Hence, proton binding to the carbon atoms had to be considered. All the complexes involving saturated carbon atoms contained a fragment bearing a five-coordinated carbon atom and an H−H bond similar to that in the methonium ion CH_5^{+}. As a rule, the most resistant complexes appeared to be those in which the bound proton was able to additionally interact with an O, N, or S atom of the amino acid. The alanine complex with the proton at the β-position provides an example of such a structure. Similar structures have also been found for other amino acids. A comparison of the data presented in Tables 4 and 7 shows that, in the case of alanine, valine, serine, and threonine, tritium is

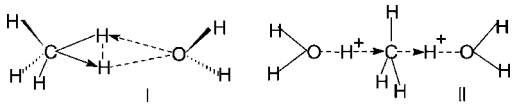

Figure 9. Transition state for hydrogen exchange between CH_4 and H_3O^+. *Ab initio* calculation of transition states of the reaction of hydrogen exchange in methane (MP2/6-311G*): I, one-center mechanism of hydrogen exchange (E_{act} 21 kcal/mol; redrawn from ref 74) II, two-center mechanism of hydrogen exchange (E_{act} 30 kcal/mol; redrawn from ref 77).

preferentially incorporated into those positions where the calculated proton affinities are greatest. Based on a comparison of the regioselectivity of the isotope exchange and affinity for the proton, it was concluded that the interaction of the proton with the aliphatic C−H bonds of these amino acids offers a qualitatively correct reflection of the observed reactivity toward SH. Therefore, it can be confidently stated that an HSCIE reaction is an electrophilic substitution reaction with SH reacting as a positively charged particle. At ambient temperatures, a proton is always bound to an electronegative atom. The proton complex with an electronodonor atom is a Brønsted-type acidic center of which the hydroxonium ion H_3O^+ can be considered the simplest representative.

Quantum chemical calculations were performed for the interaction of organic compounds with the acidic center represented by the hydroxonium ion H_3O^+. Such an interaction was earlier believed to constitute a synchronous proton transfer taking place with the involvement of two catalytic centers. The conventional reaction mechanism of hydrogen exchange between H_3O^+ and methane requires that two water molecules should be involved (Figure 9). The activation energy of this kind of reaction was found to be 30 kcal/mol (MP2/6-311G*), with an inversion of configuration of the carbon atom taking place in this case.[77] Since hydrogen isotope exchange in a HSCIE reaction proceeds with retention of configuration of the asymmetrical carbon atoms, this excludes the use of the two-center mechanism of hydrogen exchange involving the H_3O^+ acidic center. Therefore, an attempt was made to discover an alternate mechanism of hydrogen substitution at the saturated carbon atom under the action of H_3O^+: one with retention of configuration. This led to a new pathway for hydrogen substitution reaction in methane involving the action of an hydroxonium ion.[74] The activation energies of hydrogen exchange between methane and the H_3O^+ ion were determined for various approximations including both the one-center and two-center mechanisms of hydrogen exchange: 39.6 (HF/3-21G), 27.7 (HF/6-31G*), and 21.0 kcal/mol (MP2/6-311G*), respectively (Figure 9).

The transition state (TS) and the local energy minimum (LM) on the potential energy surface were also calculated with complete geometry optimization using the MP2/6-31G* method[78] as well as with Dunning's correlation basis[79] (MP2/aug-cc-pVDZ) (Table 8). Changes in bond lengths and total energy for the one-center methane−hydroxonium ion interaction are shown in Figure 10. It can be seen that hydrogen exchange involves a synchronous mechanism possessing a transition state with a pentacoordinated carbon. The hydrogen atoms being exchanged draw closer to one another, thus allowing a chemical interaction that leads to an additional stabilization of the TS.

For the $CH_4 + H_3O^+$ reaction, it was found that the transition complex (IV) is structurally close to the CH_5^+ cation. The H5−H6 distance in TS IV and in the CH_5^+ cation, calculated at the same (MP2/6-31G*) theory level, was 0.929 and 0.949 Å, respectively. The distances between the C atom and exchanging H atoms in TS 4 and in the CH_5^+ cation are 1.184, 1.189 and 1.190, 1.192 Å, respectively. The effective total charge of the CH_5 fragment in complex IV is +0.92 au.[75] Thus, these results indicate that the structure of the transition states formed according to the one-center mechanism of the hydrogen exchange reaction involving H_2 and CH_4 in the H_3O^+ acidic center, as well as the charge distributions in these systems, are rather close to those characteristic of the H_3^+ and CH_5^+ ions. Because of this, the above transition states can be represented as cations bonded to a water molecule. The reaction enthalpies for proton transfer from the H_3O^+ ion to the H_2 and methane molecule, respectively, are 63 and 35 kcal/mol. It appears therefore that these reactions are extremely hampered, whereas the formation of a TS with a close structure and charge distribution can occur with relative ease. Therefore, the one-center mechanism[74] agrees with the substitution stereochemistry observed in HSCIE reactions as well as involving smaller activation energies compared to the well-known two-center mechanism for the reaction of the hydroxonium ion with saturated organic compounds.

Molecules of water adsorbed onto the catalyst surface convert to new acidic catalytic centers under the action of

Table 8. Calculated Total Energies (E_{tot}) of Molecular Systems and Transition States of the Hydrogen Exchange Reaction between CH_4 and the H_3O^+ Ion for Different Approximations[a]

	E_{tot}, au	
system	MP2/6-31G*	MP2/aug-cc-pVDZ
H_2O	−76.1968	
CH_5^+	−40.5364	
H_3O^+	−76.4751	−76.5263
CH_4	−40.3370	−40.3676
LM	−116.8265	−116.9121
TS	−116.7806	−116.8744
ΔH_{LM}, kcal/mol	−9.97	−11.41
E_{act}, kcal/mol	18.82	12.23

[a] Redrawn from ref 75.

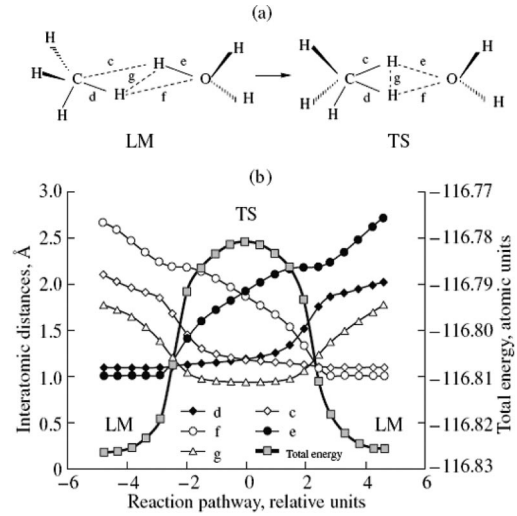

Figure 10. *Ab initio* quantum chemical calculation of hydrogen exchange between methane and a model acidic center. (a) Transition state (TS) of the reaction between CH_4 and H_3O^+ and the intermolecular complex (LM) of these compounds. (b) Pathway of the reaction between CH_4 and H_3O^+. Changes in the lengths of bonds c, d, e, f, and g and the total reaction energy by the method MP2/6-31G*. Redrawn from ref 75.

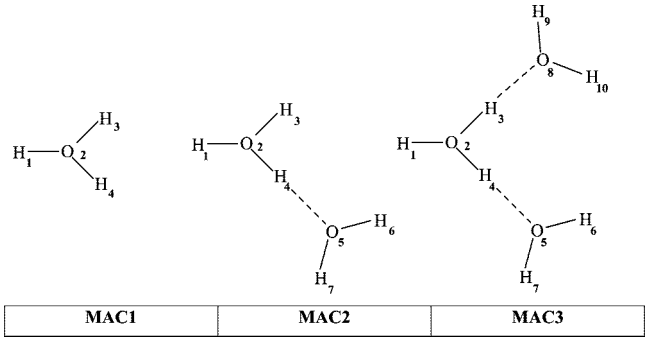

Figure 11. Structure of model acidic centers. Redrawn from ref 80.

Table 9. Calculated Characteristics of MAC1−MAC3: Bond Length (*R*), Effective Atom Charge (*q*), Total Energy (*E*), and the Energy of Proton Abstraction from MAC Including Zero-Point Vibrational Energies (PA)[a]

	model acidic center		
parameter	MAC1	MAC2	MAC3
R(H1−O2), Å	0.991	0.979	0.978
q(H1)	0.570	0.520	0.510
q(O2)	−0.709	−0.825	−0.838
E, au	−76.4776	−152.4103	−228.6124
PA, kcal/mol	163.1	196.6	220.7

[a] Redrawn from ref 80.

SH. *Ab initio* calculations were used to study the model acidic centers (MACs) represented by the $(H_2O)_nH^+$ clusters (Figure 11). All three model structures are positively charged. Some of the calculated MAC parameters are listed in Table 9.[80] The calculated proton affinity for MAC1 was found to be 163.1 kcal/mol (MP2/6-31G*; including zero-point vibration energies), which is in close agreement with the experimental value for the gas phase (165.0 kcal/mol[81]). The H4 atom in the structure of MAC2 is situated equidistant from the O2 and O5 atoms. The distance between the oxygen atoms O2−O5 calculated for this structure was found to be 2.419 Å. This is in excellent agreement with the corresponding distances for the $H_5O_2^+$ ion in heteropolyacids, which, according to the neutron diffraction data,[82] is found to be 2.414 Å. The distance between the oxygen atoms in the $(H_2O)_2$ dimer is substantially larger and equals 2.929 Å. *Ab initio* calculations[83] showed that interactions of the water dimers and the bridge hydroxyls in zeolites could result in the formation of $H_5O_2^+$ adsorbed ions and uncharged $(H_2O)_2$ clusters.

The study of the interaction of water with zeolites has been reported in many papers.[84−88] The probability of the formation of the hydroxonium ion as well as $(H_2O)_nH^+$ ions was estimated. Recently, it was shown that the introduction of an organic solvent adsorbed onto the zeolite could significantly change its acid properties.[89] The carbenium ions formed in zeolites are one of the key problems encountered in heterogeneous catalysts.[90,91] The Brønsted acid centers in solid catalysts are responsible for the formation of protonated forms and for the occurrence of reactions involving the formation of carbenium ions on these forms.[92,93] To date, processes that accompany hydrogen spillover involving heteropolyacids and sulfonated metal oxides remain largely unstudied.

Atomic positive charges, *q*(H), decrease on going from H_3O^+ to $(H_2O)_2H^+$ and even further to $(H_2O)_3H^+$. The enthalpies of interaction of H_2O with H_3O^+ and $(H_2O)_2H^+$ are 40.0 and 28.7 kcal/mol, respectively. As seen from the data presented in Table 9, the energies for proton abstraction increase substantially when the model acidic center is changed from MAC1 to MAC2 and even further when it is MAC3. They exceed the corresponding values for aluminum oxide catalysts such as zeolite HZSM (284 kcal/mol[94]). The MAC1−MAC3 centers are more acidic than the bridge OH groups of aluminosilicates. Therefore, MAC1 can be regarded as a superacidic center, MAC2 as a strong acidic center, and MAC3 as a medium-level acidic center. Many catalytic reactions on solid catalysts are known to proceed with high selectivity and in a preferred direction in the presence of trace amounts of water, hydrogen, and platinum metals. The new Brønsted acidic centers, arising due to hydrogen spillover, can be described as $(H_2O)_nH^+$. The model acidic centers MAC1−MAC3 can probably exist in aluminosilicates under hydrogen spillover conditions.

Table 10. Calculated Data for Benzene and Ethylene Complexes with MAC1−MAC3: Bond Length (*R*), Total Energy (*E*), and Enthalpy of Complexation (Δ*E*) of Benzene and Ethylene with MAC1−MAC3 (Including Zero-Point Vibrational Energies)[a]

		complex of the ligand with the acidic center		
substance	characteristics	MAC1	MAC2	MAC3
benzene	*R*(H1−O2), Å	1.783	0.997	0.994
	R(H1−C), Å	1.159	2.267	2.168
	E, au	−154.7941	−384.2210	−460.4566
	Δ*E*, kcal/mol	−22.0	−16.5	−12.1
ethylene	*R*(H1−O2), Å	1.940	2.092	2.159
	R(H1−C), Å	1.059	1.016	1.002
	R(C═C), Å	1.350	1.347	1.345
	E, au	−154.7941	−231.0402	−307.2767
	Δ*E*, kcal/mol	−20.1	−11.1	−7.3

[a] Redrawn from ref 80. *R*(H1−C) is the minimum distance between acid hydrogen and benzene ring carbon atoms.

Complete proton transfer from a Brønsted acid center to an organic substrate molecule is possible. The probability is determined by both the strength of the acid center and the proton affinity of the molecule. The theoretical proton affinities of benzene, *p*-toluene, and ethylene are 183.6, 191.0, and 162.3 kcal/mol (MP2/6-31G*; including zero-point vibration energies), respectively (Table 10)[80] whereas their experimental values are 180.0, 187.7, and 162.6 kcal/mol, respectively.[81]

The proton affinities of this series of compounds were compared with the proton abstraction energies of the MAC1−MAC3 acid centers. An analysis of the C−H bond lengths calculated for the arenonium ions shows that shorter C−H distances and lower effective charges on hydrogen correspond to proton addition at the position with the strongest proton affinity. A comparison of the proton affinities with the energies of proton abstraction for the model acid centers shows that the proton affinities of the aromatic molecules under consideration exceed the energy of proton abstraction from MAC1. Hence, in this case, we must expect complete proton transfer to the organic substrate. This is substantiated by calculations. For MAC2, the energy of proton abstraction is higher by 10−15 kcal/mol than the proton affinities of the aromatic molecules. We cannot therefore expect complete proton transfer from MAC2. Complete proton transfer is even less probable from MAC3 because the energy differences amount to ∼40−50 kcal/mol.

The most important calculated characteristics for the benzene complexes with MAC1−MAC3 are listed in Table 10. The interaction of MAC1 with benzene causes complete

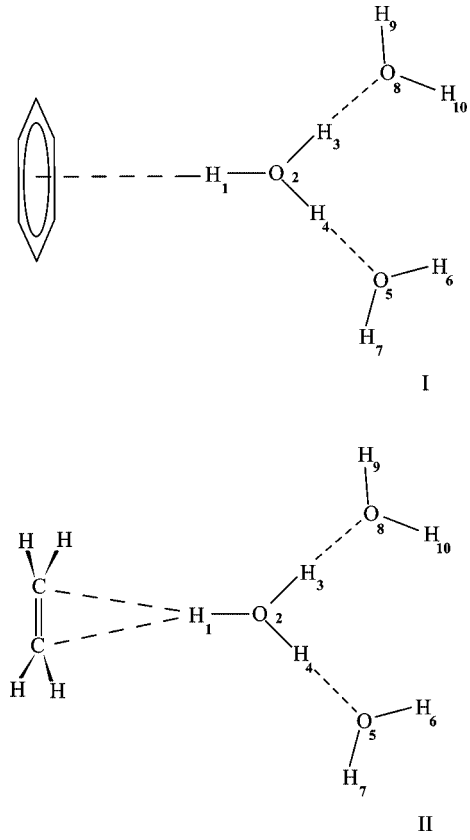

Figure 12. Structure of benzene (I) and ethylene (II) complexes with the model acidic center MAC3 (MP2/6-31G*). Redrawn from ref 80.

proton transfer from MAC1 to the aromatic system. The transferred proton forms a coordination bond with the MAC1 residue to produce a fairly strong molecular complex. Two hydrogen atoms of MAC2 and one hydrogen atom of MAC3 form π-coordination bonds with benzene (Figure 12). The energy of complex formation (ΔE) between benzene and the model acid centers decreases in the series $n = 1, 2, 3$. An approximately linear dependence on the energy of proton abstraction (PA) from the corresponding model acid centers is observed. For benzene, this dependence has the following form: $\Delta E = 0.153(\mathrm{PA}) - 47.23$ kcal/mol.

Extrapolating this ΔE(PA) dependence to the energy of proton abstraction from zeolite HZSM (284 kcal/mol[94]) yields a −3.7 kcal/mol interaction energy between benzene and this zeolite. This estimate is close to the calculated energy of complex formation between benzene and the $(OSiH_3)_3Si-OH-Al(OSiH_3)_3$ model zeolite cluster. These calculations, using the density functional method, show that benzene forms stable complexes with the model zeolite cluster; these complexes have a symmetrical structure, and the enthalpy of their formation is −1.5 kcal/mol.[92] It also follows from our calculations that the structure of the benzene complexes with the model acid centers changes from σ-(MAC1) to π-(MAC3) as the acidity of MACs decreases.[80]

When a proton adds to the ethylene, a π-complex is produced. Interaction of this type is only characteristic of unsubstituted ethylenes. This π-type addition is characteristic of ethylene interactions with MAC1−MAC3 (Figure 12). When ethylene interacts with MAC1, no hydrogen transfer from MAC1 to ethylene occurs at the initial stage, that is, during the molecular complex formation. The ethylene plane is oriented normally to the H1−O2 bond. Some calculated

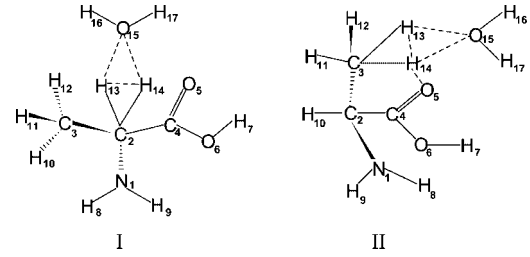

Figure 13. Transition state structures for the hydrogen exchange reaction between H_3O^+ and alanine for substitution in the αC (I) and βC (II) positions. Redrawn from ref 75.

characteristics of a series of ethylene complexes with MAC1, MAC2, and MAC3 are listed in Table 10. The distances between the active proton of the MACs and the ethylene carbon atoms increase, and the O−H distance decreases as we go from MAC1 to MAC2 and to MAC3. The data in the table show that the energy (ΔE) of ethylene interactions with MACs' centers monotonically decreases from MAC1 through MAC3. The ΔE energy is related to the proton affinity (PA) of the MACs by the following simple equation: $\Delta E = 0.2559(\mathrm{PA}) - 64.69$ kcal/mol.

Extrapolating this ΔE (PA) dependence to the energy of proton abstraction from the zeolite HZSM (284 kcal/mol[94]) yields the interaction energy between ethylene and this particular zeolite. The interaction energy of ethylene with the zeolite is +8 kcal/mol and repulsive. These estimations show that complex formation on acidic centers of the zeolite HZSM is possible only with benzene. As our calculations have shown,[80] the enthalpy ratio of the benzene/ethylene complex formation with the acidic centers changes and depends on the power of the acidic centers. For superacidic centers, the stability of the benzene and ethylene complexes is equal. In the case of the medium strength acidic centers, the interaction with benzene appears to be stronger. However, the interaction of ethylene is possible with the acidic centers formed on the surface of a zeolite under the action of SH. This result is relevant in understanding the importance of the role of SH in the reaction mechanism of organic compounds on acidic centers of catalysts.

Ab initio calculations using the MP2/6-31G* method were performed for the interactions between Ala and H_3O^+ as the model acidic center.[75] The resulting transition states are depicted in Figure 13. The calculated activation energies for H-Cα and H-Cβ were found to be 19.6 and 10.5 kcal/mol (MP2/6-31G*), respectively. The activation energy for H-Cα appears to be rather close to the corresponding value for methane (19.8 kcal/mol; MP2/6-31G*). According to the proposed mechanism, hydrogen exchange occurs much more easily in the β-position than in the α-position. Interaction between the substituted hydrogen and the carbonyl oxygen was evident in the transition state of the hydrogen exchange at H-Cβ (Figure 13). In the transition state, the H14−O5 distances were found to be 2.164 Å and 2.958 Å for hydrogen exchange at H-Cβ and H-Cα, respectively. From the analysis of the electron distribution in the TS for this alanine exchange reaction,[75] it follows that the interaction between the O atom of the carboxyl group and the H_2 group is mainly Coulombic in nature. In fact, the charge on the H13−H14 grouping is +0.83 au, whereas the effective O5 carbonyl charge is −0.55 au. It was concluded that the most probable reason for the high reactivity of the Ala methyl group is the interaction, in the transition state, between the carbonyl oxygen and the exchanging hydrogen atom at Cβ. These *ab initio* results

Table 11. Tritium Distribution in Hydroxyproline from the HSCIE Reaction at 150 °C and the *ab Initio* Calculation of the Activation of the Hydrogen Exchange Reaction by RHF/6-31G*[a]

exchangeable hydrogen	tritium inclusion, %	E_{act}, kcal/mol
H-C2	9	23.59
H_α-C3	6	23.72
H_β-C3	1	26.17
H-C4	4	25.57
H_α-C5	59	18.07
H_β-C5	21	22.03

[a] Redrawn from ref 78. E_{act} of the exchange reaction in methane is 27.7 kcal/mol (RHF/6-31G*).

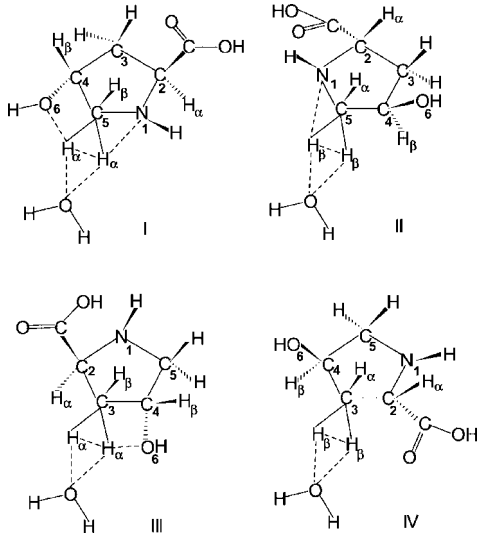

Figure 14. Transition states (TS) for the reaction of L-hydroxyproline with the acidic center H_3O^+; *R* denotes the distances between the atoms in angstroms. Hydrogen exchange at carbon atoms: (I) TS for H_α-C5, $R(H_\alpha-N_1) = 2.11$, $R(H_\alpha-O_4) = 1.82$ Å; (II) TS for H_β-C5, $R(H_\beta-N_1) = 2.10$, $R(H_\beta-O_4) = 3.14$; (III) TS for H_α-C3, $R(H_\alpha-N_1) = 3.27$, $R(H_\alpha-O_4) = 1.96$; (IV) TS for H_β-C3, $R(H_\beta-N_1) = 2.26$, $R(H_\beta-O_4) = 3.47$. Redrawn from ref 78.

are in good agreement with experimental data on the regioselectivity and stereoselectivity for the solid-state isotope exchange reaction of hydrogen by spillover-tritium.[50]

The results in Table 11 are for the experimental study of isotope exchange in L-hydroxyproline (L-Hyp) and the theoretical calculations for the exchange ability of the L-Hyp H atoms.[95] The structures of the HSCIE transition states formed in L-Hyp are shown in Figure 14. The activation energy for the interaction of the model acidic center with the amino acid was found using the *ab initio* RHF/6-31G* method. These data show that in HSCIE a correlation exists between the reactivity of the amino acid C−H bonds and the calculated hydrogen exchange activation energy. The greater the ability of hydrogen to be substituted by tritium, the smaller the E_{act}, as found in the *ab initio* calculations. The capability of H to be substituted increases with additional transition state stabilization. Electronic interaction between the hydrogen atoms and any electron-donating atoms participating in the reaction provides this stabilization and, hence, a decrease in the activation energy. The hydroxyproline Hα-C5 exhibits the highest reactivity. In this case, the reacting H appears to be drawn close to both the O6 atoms and N1. Interaction with the hydroxyl group at C4 becomes impossible for Hβ-C5, and the TS stabilization occurs on N1 only. The Hα at C3 can interact only with O6 in the TS whereas in the case of Hβ all the heteroatoms are situated too far away for interaction and, hence, stabilization of this particular

Table 12. Relative Reactivities of C−H Bonds in Amino Acids with Respect to the Methyl C−H Bonds in L-Valine (R_{ref})[a]

	position							
	Cα		Cβ		Cγ		Cδ	
amino acid	R_{ref}	E_{act}	R_{ref}	E_{act}	R_{ref}	E_{act}	R_{ref}	E_{act}
Ala	0.14	37.0	1.09	29.7				
Val	0.26	38.4	0.26	25.2	1.00	21.7		
Ser	2.65	23.9	0.57	30.5				
Thr	0.89	27.2	0.44	26.5	1.21	18.1		
Pro	0.37	36.5	0.12	31.2	0.08	33.4	1.67	29.7

[a] Activation energy (E_{act}, kcal/mol) for HSCIE reaction between amino acid H−C and model acidic center H_3O^+ (HF/3-21G). Redrawn from ref 96.

transition state. Data confirming the proposed solid state isotope exchange mechanism have also been obtained from *ab initio* calculations of the interaction of Val, Pro, and Thr with the H_3O^+ acidic center (Table 12).[96] In the amino acid, a smaller reaction activation energy, obtained from *ab initio* calculations for the one-center synchronous mechanism of hydrogen exchange, and which includes stabilizing interactions of the electron-donating atoms N and O with the exchanging hydrogen atoms, is found to correspond to those positions showing greater reactivity. These combined results, therefore, confirm the relevance of the one-center synchronous mechanism of hydrogen exchange to the observed reactivity of this series of amino acids in the HSCIE reaction. We hope that this one-center mechanism for the reaction of organic compounds with Brønsted-type acidic centers can be applied to further spillover-hydrogen studies.

The substitution of isotopic atoms into a compound clearly gives rise to isotope effects, and the investigation of thermodynamic and kinetic isotope effects is an important tool in studying the mechanisms of such chemical reactions. It is well-known that considerable isotope effects are evident in vibrational spectra. Changes in the characteristic frequencies of isotopomer molecules depend strongly on the relative change in the weight of the isotopic atoms. Conversely, isotopic shifts in the fluorescence and phosphorescence spectra of deuterium-substituted organic compounds have not yet been observed. Both fluorescence and phosphorescence spectroscopy of tryptophan residues are widely used for the analysis of structure and complexation in proteins.[97] Tryptophan is especially useful, because its fluorescence is so sensitive to the molecular environment. Unfortunately, the fact that it has complex photophysics has made structural analysis based on tryptophan fluorescence quite challenging. Deuterium isotope effects on the fluorescence quantum yield for tryptophan have been analyzed.[98] Isotopic shifts in the UV-absorbance spectra of tritium-substituted tryptophan have been observed for the first time.[99,100] A HSCIE reaction was used to prepare uniformly tritium-labeled tryptophan.[48] Figure 15 shows the distribution of the isotope label in L-[^{3}H]Trp. There are two maxima in the tryptophan UV-absorption spectrum at 280 and 220 nm, corresponding to the electronic transitions I_1 and I_3 (Table 13).

The restricted Hartree−Fock method (RHF) was used for tryptophan calculations. For the isotope-substituted isomers, the restricted Becke−Lee−Young−Parr modification (RB3LYP) was used for the density functional theory,[101] as well as the configuration interaction (RCIS) method.[102] The Dunning−Hay D95 atomic basis set was used both for the optimization of the geometry and for the calculation of the normal vibration frequencies. Excited states were calculated using the configuration interaction method RCIS and the D95 basis set.

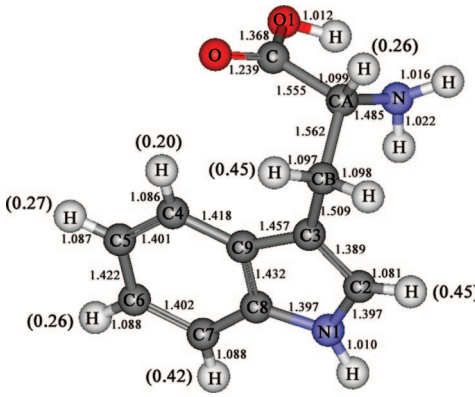

Figure 15. The structure, geometric parameters, and degree of tritium−hydrogen substitution of tryptophan (in brackets). Redrawn from ref 99.

Table 13. Isotopic Shift (δ) of Zero-Point Energy Correction Levels (ZPE) for Ground and Electronic Excited States of [2,7-^{3}H]Trp[a]

spin state	level of spin state,[b] I	ZPE, a.u. ZPE(T)	ZPE, a.u. ZPE(H)	isotopic shift, δ,[c] kcal/mol
singlet	0	0.225315	0.235311	6.2726
singlet	1	0.217958	0.227712	6.1207
singlet	2	0.223848	0.233622	6.1333
triplet	0	0.218384	0.227492	5.7154

[a] Redrawn from ref 100. [b] Ground ($I = 0$) and electronic excited ($I = 1, 2$) states. [c] $\delta = \mathrm{ZPE(H)}_I - \mathrm{ZPE(T)}_I$.

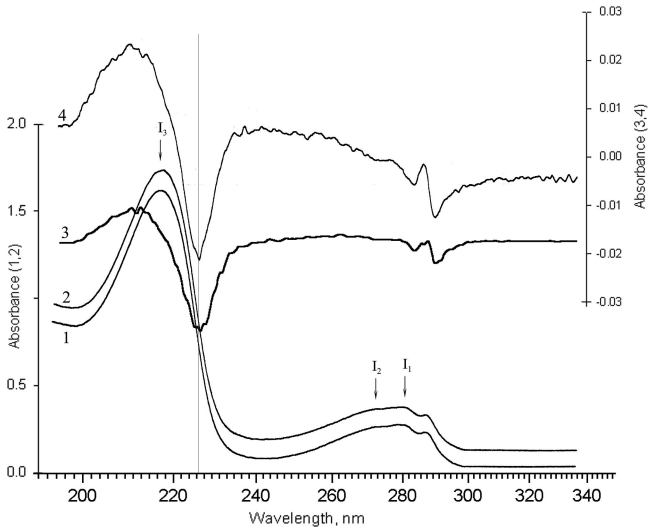

Figure 16. UV spectrum of (1) L-[^{1}H]tryptophan and (2) L-[^{3}H]tryptophan; (3) the first derivative of the L-[^{1}H]tryptophan UV spectrum; and (4) the differential UV spectrum of L-[^{3}H]tryptophan against L-[^{1}H]tryptophan. Redrawn from ref 100.

A comparison of the L-[^{3}H]Trp and L-[^{1}H]Trp UV spectra showed a short-wavelength shift of the absorption maximum in the tritium-substituted compound corresponding to an energy of 130 cal/mol for the electronic transition (Figure 16). The shifts of all the allowed electronic transitions were shown to shift toward the short-wavelength region. Shifts varied from 152 cal/mol for the first singlet−singlet transition (within the 280 nm region) to 242 cal/mol for the third transition (within the 220 nm region) and to 557 cal/mol for the singlet−triplet transition (Table 13).

Isotopic shifts in the electronic spectra of tryptophan during deuterium substitution were analyzed for [indole-$^2H_5$]Trp.[103] Figure 17 shows a part of the UV-absorption spectrum (a.1),

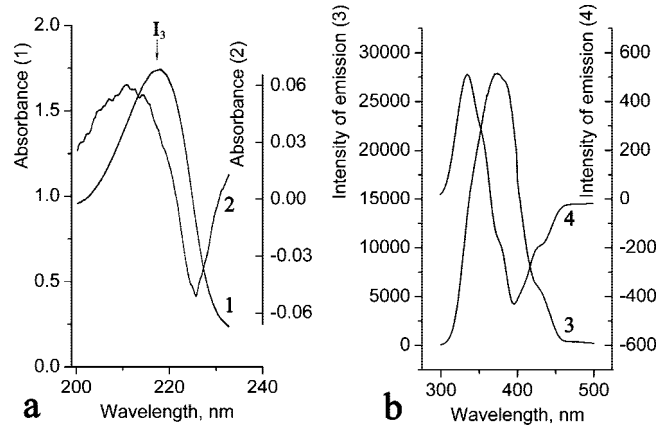

Figure 17. Experimental analysis of isotopic effects for electron transitions of tryptophan. Part of the UV-absorption (a.1) and fluorescence (b.3) spectra of [^{2}H]Trp. Differential UV-absorption (a.2) and fluorescence (b.4) spectra for [^{2}H]Trp with regard to [^{1}H]Trp. Redrawn from ref 103.

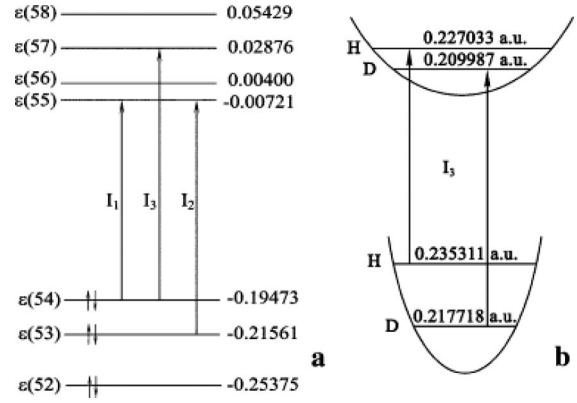

Figure 18. Theoretical analysis of isotopic effects for electronic transitions of tryptophan. (a) Diagram of one-electron levels for tryptophan. (b) Electronic transition energy in X-H compound. Zero-point oscillation energies for [^{1}H]Trp-(H) and [^{2}H]Trp-(D) of the ground and excited states. Redrawn from ref 103.

the fluorescence spectrum (b.3), the differential UV-absorption spectrum (a.2), and the differential fluorescence spectrum (b.4) of [^{2}H]Trp. The short-wave isotopic shift of the band at 220 nm in [^{2}H]Trp was calculated for that part of the differential UV spectrum corresponding to the electronic transition I_3. It was found to be 0.62 nm or 360 cal/mol. The [^{2}H]Trp (b.3) fluorescence spectrum reached its maximum at 369 nm. The short-wave shift was found to be 1.0 nm or 210 cal/mol. For calculating the isotope shifts of the I_1, I_2, and I_3 transitions, zero-point energy corrections (ZPC) were determined for the electronically excited states of the triplet and singlet tryptophan molecules (Figure 18). The numerical values of the ZPC are the energy distances from the bottom potential curves to the first vibration level. The ZPC for the ground states of [^{2}H]Trp is 11.0398 kcal/mol lower than that of [^{1}H]Trp and is 10.6965 kcal/mol lower than that of [^{1}H]Trp for the third excited state of [^{2}H]Trp. So, the calculated isotopic shift of the I_3 transition energy in [^{2}H]Trp is 343 cal/mol. There is good agreement between the experimental (360 cal/mol) and calculated isotopic shifts of the band at 220 nm and the transition energy I_3. In the phosphorescence spectrum of tryptophan, the calculated isotopic shift for the singlet−triplet excitation is 503 cal/mol.

It was found that the calculated isotopic shift for electronic transitions in Trp depends on the positions of the deuterium

Table 14. Calculated Isotopic Shifts for Electronic Transitions from Ground to Singlet (I_1, I_2, I_3) and Triplet (I_T) Excited States for Different Positions of Deuterium Label in Trp[a]

deuterium substituted tryptophan	isotopic shift for electronic transitions, cal/mol			
	I_1	I_2	I_3	I_T
[1-^{2}H]Trp	14	11	169	85
[2-^{2}H]Trp	58	42	118	365
[4-^{2}H]Trp	56	50	73	100
[5-^{2}H]Trp	29	56	60	90
[6-^{2}H]Trp	52	60	13	107
[7-^{2}H]Trp	48	56	80	85
[α,β,β-^{2}H]Trp	4	2	45	14

[a] Redrawn from ref 103.

label (Table 14). The greatest isotopic effect for singlet−triplet transitions corresponds to [2-^{2}H]Trp, just as the highest isotopic effect for singlet−singlet transitions I_3 corresponds to [1-^{2}H]Trp. The substitution of 3 H−C atoms into the aliphatic part of Trp exhibits only weak isotopic effects as for singlet−singlet transitions I_1 and I_2, as for the singlet−triplet transition. The measurement of isotopic shifts for electronic transitions in aromatic, heteroaromatic, and metallo-organic compounds has the potential to be utilized as a new informative method for the investigation of chemical bonds and complexation. The origin of this phenomenon is attributed to the difference in the zero-point energy of the ground and excited states of the isotope-substituted molecule.

4. HSCIE Reaction with Peptides and Proteins

The solid state isotope exchange reaction conducted at elevated temperatures was shown to be effective not only for the introduction of isotopes into stable compounds such as amino acids but also for peptides and proteins.[104−106] An important feature of the HSCIE with peptides is that the reactivity of the peptide fragment can change with any change in the structure and conformation of the peptide chain.[107] This was shown to be the case for the structurally related enkephalins; namely, the endogenous opioid peptide [Leu^5]-enkephalin (LENK, Tyr-Gly-Gly-Phe-Leu) and its synthetic analogue dalargine (DALG, Tyr-D-Ala-Gly-Phe-Leu-Arg). The tritium labeled peptides were produced at 180 °C, and they showed similar molar radioactivity values, 120 and 138 Ci/mmol for LENK and DALG, respectively. Figure 19 shows MS analysis of [^{2}H]DALG, and Table 15 shows the distribution of tritium in [^{3}H]DALG and [^{3}H]LENK.

As evidenced by the data, the behavior of these peptides resembles closely the reactivity of their fragments. In the Tyr1 residues, for example, the most facile exchange proceeds in the *ortho*-position to the OH-group of the aromatic ring. This position is characterized by the largest affinity to the proton and facilitates interaction with the electrophilic acidic catalytic center that is created in HSCIE reactions under the SH action. Pairwise comparison of the reaction ability of the C−H bonds in the enkephalins studied showed that although the substitution ability of H-C2, H-C3, and H-Cβ is close in the Tyr1 fragments, for Tyr1 in the tritium exchange with H-Cα, an order of magnitude larger difference was observed. A similar increase in reactivity for the H-Cα in DALG compared with LENK was also observed in the Phe4 and Leu5 fragments. The reaction ability of H-Cβ and C−H in the aromatic moiety of Phe4 is similar in LENK and DALG. The considerable difference in the amount of tritium incorporated into the Phe4 fragments of these peptides is accounted for by the different reactivity of H-Cα. Almost

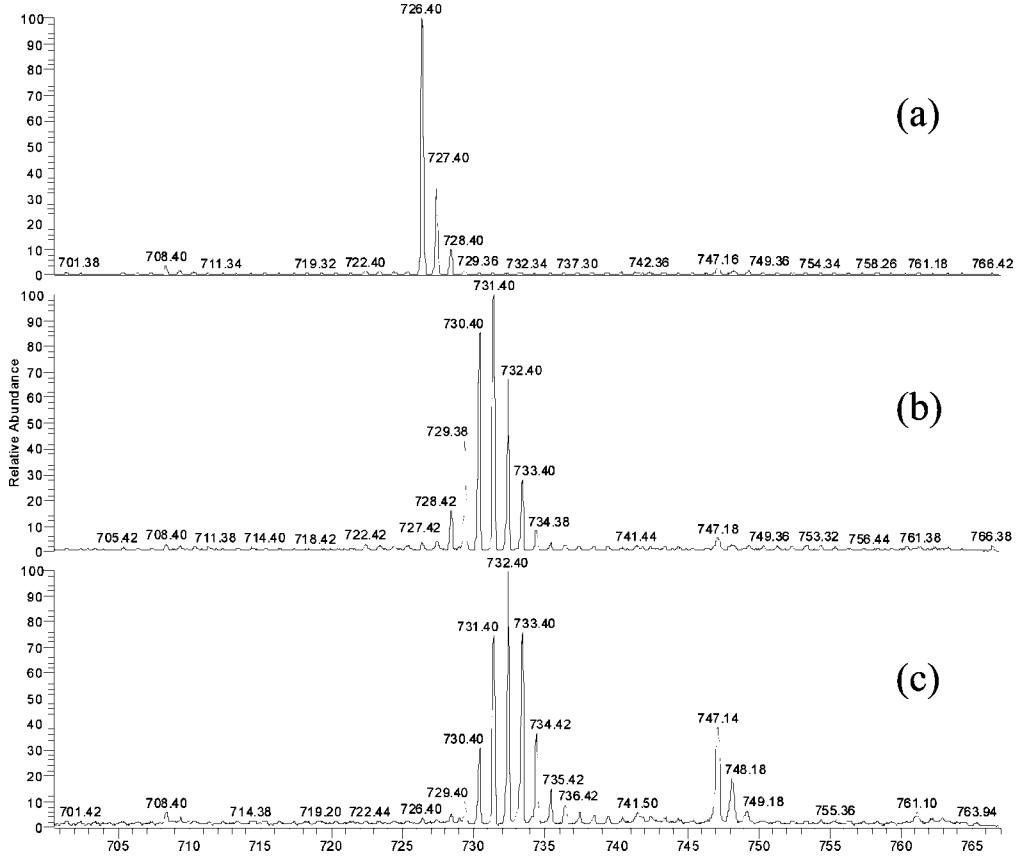

Figure 19. MS analysis with an ion trap of [G-^{1}H]dalargine (a) and [G-^{2}H]dalargine (b), (c) with average incorporation of 4.4 and 5.9 deuterium atoms, respectively. Redrawn from ref 58.

Table 15. Distribution of Isotope Label (%) According to ^{3}H NMR[a] after HSCIE Reaction in [^{3}H]Enkephalins[b] at 180 °C for 20 min[c]

amino acid residue	tritium portion, %		label position in residue	DALG		LENK	
	DALG	LENK		δ, ppm	portion of ^{3}H, %	δ, ppm	portion of ^{3}H, %
Tyr1	27.1	28.0	CαH	4.15	4.6	4.20	0.5
			Cβ2H	3.09	1.3	3.08	1.8
			C2,6H2	7.17	1.5	7.20	2.5
			C3,5H2	6.87	19.7	6.91	23.1
Gly2		30.5	CαH2			3.85	30.5
Gly3	30.5	31.8	CαH2	3.80	30.5	3.78	31.8
Phe4	20.0	9.1	CαH	4.60	14.3	4.60	1.5
			Cβ2H	3.08; 2.95	2.0	3.12; 2.96	2.9
			C2,6H2	7.29	1.0	7.29	1.3
			C3,5H2	7.40	2.0	7.40	2.4
			C4H	7.35	0.7	7.35	1.0
Leu5	6.3	0.6	CαH	4.30	6.3	4.19	0.6
Arg6	16.1		CαH	4.29	14.8		
			Cβ2H	3.10	1.3		

[a] 640 MHz in D_2O at pH 7.0, Varian UNITY-600. [b] [Leu5]Enkephalin (LENK) and Dalargine (DALG) with molar radioactivities of 120 and 138 Ci/mmol, respectively. [c] Redrawn from ref 107.

70% of the H^1 substitution for H^3 was observed for Phe4 H-Cα in DALG. On the other hand, the degree of substitution in Phe4 H-Cα in LENK was only 6%. Since all these peptide structures are similar, the probable cause of such a dramatic increase in the reactivity of H-Cα in all the DALG amino acids can possibly be an additional charge present on the guanidine group of Arg6 in DALG. This results in a conformational change of the peptide chain. The Gly3 residues in DALG and LENK showed high reactivity. Under selective HSCIE conditions, the tritium substitution degree for hydrogen in these residues went from 65 to 70%. It was found out that the isotope exchange intensity in Gly2 in LENK was approximately the same as that found in Gly3. The HSCIE reaction makes it possible to produce uniformly tritium-labeled peptides[108] for use both in receptor binding analysis[109−112] and for the determination of their peptidase biodegradation paths *in vivo* and *in vitro*.[113−115]

It has been shown that these uniformly tritium labeled peptides completely retain their biological activity.[116,117] The theoretical analysis of hydrogen exchange in the CtxG1 polypeptide revealed some important HSCIE features regarding the influence of peptide chain mobility on the reactivity of amino acids (Figure 20; Table 16). It is well-known that HSCIE reactions in free amino acids have comparable rates. Therefore, it might be expected that tritium would be found in all the CtxG1 residues. As the results in Table 16 show, however, there was no isotope exchange detected in the Ala fragment of Asn4-Pro5-Ala6.[107] The lowered reactivity of these residues is probably due to the three-dimensional features of the CtxG1 structure. The isotope label distribution in the peptide chain is probably determined by the reactivity of the C−H bonds of the individual amino acid residues as well as by their accessibility to SH. The accessibility was estimated from the proportion of van der Waals surface accessible for interaction with H_2O. This parameter was determined using the MOLMOL program.[118] The reactivity of the C−H bonds in CtxG1 was analyzed in the CtxG1 fragments by the *ab initio* quantum-chemical calculation of the HSCIE transition state and by the Hartree−Fock method.

The absence of ^{3}H in Pro5 and Asn4 might be accounted for by limited access to the most reactive positions in these amino acids. The CβH of Pro5 as well as the CαH and CβH of Asn in CtxG1 were shown to possess low accessibility. However, even though the Ala6 methyl group is completely open, tritium fails to incorporate into this part of the molecule

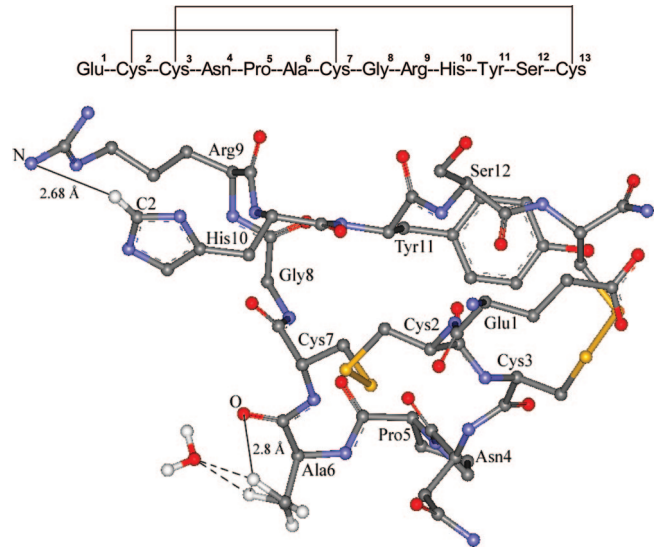

Figure 20. Spatial structure of α-conotoxin G1 (CtxG1) and transition states for the HSCIE reaction in Ala6 and His10 in CtxG1. Redrawn from ref 107.

(Table 16). This indicates that although the accessibility of some peptide part is necessary, it is not necessarily a sufficient precondition for the HSCIE reaction to proceed. The fact that the Ala amino acid is located within the Asn4-Cys7 fragment which has a more rigid conformation than the remaining part of the CtxG1 molecule is one of the particular features of the Ala6 structure. This results in a typical α-spiral conformation for Ala6.[119]

In order to carry out quantum-chemical calculations for the isotope exchange reaction path, the geometry of the heavy atoms in the model fragment CH_3–C(O)–NH–CαH(CH_3)−C(O)−NH_2 was recorded in correspondence with the conformation of the Pro5-Ala6-Cys7 fragment from CtxG1. The geometry of the remainder of the reaction complex was completely optimized by calculating the geometric parameters for the transition state of the model fragment. The calculated activation energy (E_{act}) for the hydrogen exchange reaction at the Ala6 atom Cβ was found to be 33.7 kcal/mol (HF/6-31G*).[107] It should be noted for comparison that the E_{act} calculated for the isotope exchange of the H-Cβ atom in free alanine is 16.6 kcal/mol (HF/6-31G*). The lower E_{act} for H-Cβ in the HSCIE reaction of free alanine can be explained by the involvement of the

Table 16. Distribution of Isotope Label in Labeled α-Conotoxin G1 Obtained by the HSCIE Reaction with Tritium at 140 °C[a]

amino acid residue	tritium portion in residue, %	label position in residue	δ, ppm	portion of tritium in position
Glu1	3.6	CγH2	2.18	3.6
Cys2	7.0	CαH	4.60	7.0
Cys3	9.2	CαH	4.65	9.2
Asn4	0			
Pro5	0			
Ala6	0			
Cys7	8.0	CαH	4.48	8.0
Gly8	2.8	CαH	3.78; 4.03	2.8
Arg9	1.8	CγH2	1.25	1.8
His10	50.6	C2H	7.70	46.6
		CαH	4.73	4.0
Tyr11	4.1	C3H, C5H	6.77	1.4
		CβH2	2.88	2.7
Ser12	3.7	CαH	4.34	3.7
Cys13	9.2	CαH	4.63	9.2

[a] Estimated according to the ^{3}H NMR spectrum (640 MHz) in D_2O at pH 7.5 and 30 °C; Varian UNITY-600 spectrometer (United States). Redrawn from ref 107.

Table 17. Chemical Shifts of Signals in the ^{3}H NMR Spectrum of Zervamycin: Their Relative Integral Intensity and Assignments[a]

amino acid residue	tritium portion in residue, %	label position in residue	δ, ppm	portion of tritium in position
Trp1	2.0	C7H	7.55	0.5
		C2H	7.42	1.5
Ile2	1.9	CαH	3.85	1.9
Gln3	38.8	CβH2	2.40	18.9
		CβH3	2.15	16.7
		CγH2	3.50	3.2
Leu8	0.8	CαH	4.42	0.8
Hyp10	10.8	CβH2	2.12	1.9
		CβH3	2.55	8.9
Hyp13	11.8	CβH3	2.54	9.3
		CγH	4.58	2.5
Pro15	33.9	CβH3	2.23	25.3
		CδH2	4.02	8.6

[a] The ^{1}H and ^{3}H NMR spectra were obtained in CD_3OD at 30 °C on a Varian UNITY-600 spectrometer (United States) at the working frequency of 600 and 640 MHz for protons and tritons, respectively. Redrawn from ref 107.

transition-state carbonyl oxygen. In this case, the distance between the carbonyl O atom and the exchanging H-Cβ atoms is only 2.16 Å. In the case of CtxG1, the high E_{act} for hydrogen exchange in the Ala methyl group is due to the rigid conformation of this part of the peptide. This hinders the interaction of the carbonyl O with H-Cβ in the transition state (the distance between O and H-Cβ is 2.8 Å). Thus, it was shown, for the first time, that, in the case of CtxG1, the limited flexibility of the peptide fragment can cause a considerable decrease in the HSCIE reaction rate under the action of SH.

According to the ^{3}H NMR spectrum for [^{3}H]CtxG1, 57% of the H-C2 His10 was substituted by tritium. Table 16 shows that imidazole His10 appears to be the most active in the HSCIE reaction of CtxG1. A similar phenomenon was previously observed in the HSCIE reaction of free histidine and its tripeptides.[48] But while the reactivity of the hydrogen atoms at C2 and C4 in the imidazole ring appears to be close in histidine and its tripeptides, the isotope exchange in the G1 α-conotoxin proceeds exclusively at C2. Probably, the participation of the CtxG1 electron-donating atoms in the stabilization of the HSCIE transition state in imidazole His10 is the reason for the high reactivity of H-C2 His10.

It is also probable that the participation of the CtxG1 electron-donating atoms in the stabilization of the HSCIE transition state in imidazole His10 is the reason for the high reactivity of H-C2 His10. Analysis of the three-dimensional structure of CtxG1, obtained from the X-ray structural analysis data, shows that only the Arg9 guanidine group can act as an electron density donor for the H-C2 imidazole ring of His10. The quantum-chemical calculation of the hydrogen exchange transition state in the CtxG1 fragment, including both Arg9 and His10, has been performed to confirm this assumption. The geometry parameters for the heavy atoms of this fragment were obtained from the X-ray structural data and used in the transition state calculations. According to these data, the distance between the exchanging atom H-C2 of His10 and the N atom of Arg9 in guanidine in the transition state was 2.68 Å, and the activation energy of this reaction was found to be very low, only 7 kcal/mol (HF/6-31G*). Therefore, it is the short distance between the imidazole ring of His10 and the guanidine of Arg9 that explains why only about half the tritium introduced into the peptide was incorporated at the H-C2 position of the His10 imidazole ring.

The results obtained for CtxG1 allow us to confidently state that the necessary condition for making the HSCIE reaction possible in these polypeptides is the participation of the electron-donating O and N atoms in the transition state stabilization. In such cases, the electron-donating atoms can belong either to the residue where the exchange takes place or to other spatially close amino acid residues. Thus, unlike isotope exchange in free amino acids, in this case spatial accessibility of the exchanging protons for interaction with the acidic centers formed under SH conditions is essential. In addition, the conformational rigidity of the peptide fragment can either facilitate or hinder the participation of the electron-donor atoms in the transition state and hence play an important role in HSCIE-polypeptide reactions.

Both theoretical and experimental studies of solid state isotopic hydrogen exchange reactions were carried out using zervamycin IIB (Ac-Trp-Ile-Gln-Iva-Ile-Thr-Aib-Leu-Aib-Leu-Hyp-Gln-Aib-Hyp-Aib-Pro-Phl, where Aib is 2-aminoisobuturic acid).[107] [^{3}H]Zervamycin IIB with a molar radioactivity of 70 Ci/mmol was obtained. Table 17 shows the distribution of tritium in the [^{3}H]zervamycin IIB. This peptide is of interest because it contains the Trp1-Leu8 fragment, which adopts an α-helical conformation (Figure 21).[120]

Hyp 10, Hyp 13, and Pro 15 all display high reactivities in zervamycin IIB. Tritium incorporation into these amino acids occurs with a high regio- and stereoselectivity at the Cβ-position in relation to CαH in the pyrrolidine ring plane. Furthermore, as the results in Figure 21 show, the HSCIE reaction takes place preferentially "on one side of the zervamycin IIB molecule". An explanation for the observed isotope distribution in this particular polypeptide might be the orientation of zervamycin IIB during the sorption onto the nonorganic support during the HSCIE reaction.

It is possible that the spatial restrictions and conformational rigidity emerging during the formation of the α-helical fragment, Trp1-Leu8, give rise to the lower reactivity displayed by the majority of its amino acids. The high degree of tritium substitution for H-Cβ in Gln3 could be related to the advantageous positioning of both the oxygen atom of the Gln3 side chain carbonyl and the nitrogen of the peptide

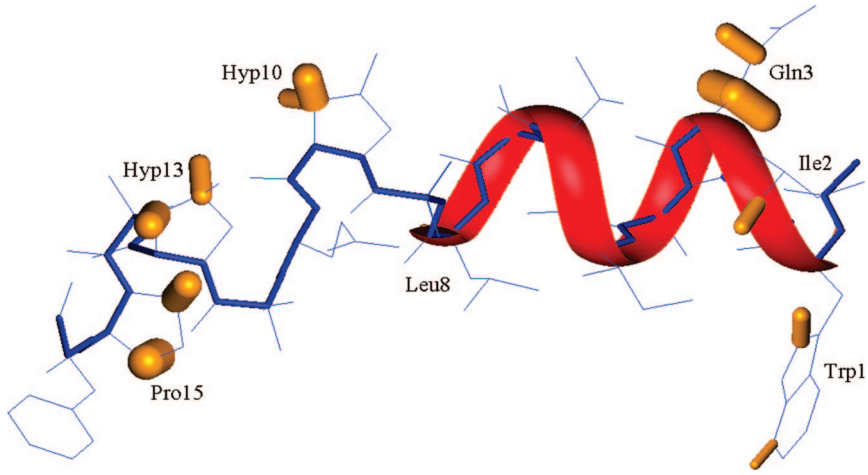

Figure 21. Spatial structure of zervamycin IIB. The broadness of the lines of the H−C bonds is proportional to the logarithm of the tritium content at HC (cf. Table 17). Redrawn from ref 121.

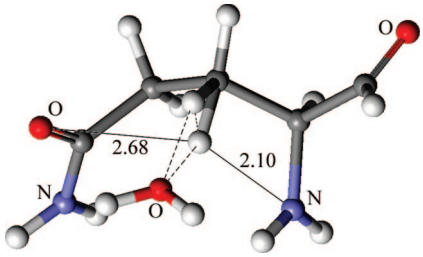

Figure 22. Calculated transition state structure for the HSCIE reaction at H-Cβ in Gln3 of zervamycin IIB (MP2/6-31G*). The distance between the exchangeable hydrogen and the amide N of the peptide bond is 2.1 Å. Redrawn from ref 121.

chain amino group, since both contribute to the progress of the HSCIE reaction. The α-helical fragment, Trp1-Leu8, has a relatively rigid conformation; therefore, in order to calculate the transition state, the geometry of the heavy atoms in the Ile2-Gln3-Iva4 fragment of the peptide chain had to be fixed with respect to its conformation. The calculated activation energy for H-Cβ in Gln3 was found to be 26.2 kcal/mol (MP2/6-31G*), whereas the E_{act} for H-Cα and H-Cγ were 30.9 and 35.3 kcal/mol (MP2/6-31G*), respectively. In Gln3 the activation energy for hydrogen exchange for H-Cβ appears to be the lowest: this is in accordance with the highest degree of protium-for-tritium exchange. Thus, the involvement of the carbonyl group of the Gin3 side chain together with the peptide chain nitrogen in the interaction with H-Cβ in Gln3 gives rise to a considerable increase in reactivity at this position (Figure 22).

The HSCIE reaction was also studied in the thermophile β-galactosidase, which was obtained from *Thermoanaerobacter ethanolicus*. This is a homodimer with a subunit molecular mass of 83 kDa. Mesophilic β-glucosidase from almonds (3.2.1.21, Sigma), which is a heterodimer consisting of subunits of 117 and 66.5 kDa was also studied.[121] The dependence of the molar radioactivity and the retention of the enzymatic activity of β-galactosidase under HSCIE reaction conditions were established (Table 18). It was shown that they behave similarly under HSCIE conditions and completely retain their enzymatic activity even at 120 °C. It is noteworthy that their thermostabilities differ by several tens of degrees under aqueous conditions. The KEM-QKE215-220 region of β-galactosidase, located on the surface of the protein globule and not involved in the secondary structure formation, exhibits the largest relative reactivity.

Table 18. Dependence of Specific Radioactivity and Retention Degree of Enzymatic Activity on the HSCIE Reaction Temperature during Production of Tritium Labeled Proteins of Thermophilic β-Galactosidase from *Termoanaerobacter ethanolicus* and Mesophilic β-Glucosidase from Almond (Sigma)[a]

	β-galactosidase		β-glucosidase	
T, °C	specific radioactivity, Ci/mmol	enzymatic activity, %	specific radioactivity, Ci/mmol	enzymatic activity, %
40	54	100	50	100
80	960	100	600	100
100	1090	100	980	100
120	1440	100	1400	100
140	2050	59	1980	45
160	3870	6		

[a] Redrawn from ref 121.

The effect of spatial interaction in protein complexes on changes in their reactivity toward SH was studied in the case of hydrogen solid state isotope exchange in bovine hemoglobin.[122] The hemoglobin is a tetramer formed by two α-subunits and two β-subunits and includes four heme molecules. Classic enzymatic trypsin hydrolysis was used to study the isotope label distribution in the polypeptides. HPLC was used to separate the resulting tritium-labeled peptide fragments obtained from the α-chain of the bovine hemoglobin (Figure 23). The reference of the peptides made by MALDI mass spectrometry was used to identify the fragments, and the radioactivity of the tripeptides was determined by liquid scintillation counting. Numbers were estimated according to the square of the corresponding chromatographic peaks: wavelength 210 nm. The ability to hydrogen exchange in the peptides was evaluated by the amount of reduced radioactivity calculated as the ratio of the radioactivity of the chromatographic peak to its area. Pairwise comparison of the adjusted radioactivity showed that by introducing the same triptic fragments of the α-subunit, either in its free form or as a protein complex, into the HSCIE reaction it was possible to determine any changes in the hydrogen exchange ability resulting from protein complex formation. Results are shown in Table 19.

A comparison of pairs of triptic fragments produced by the isotopic exchange with hemoglobin or a free polypeptide reveals that the reactions proceed differently. It was found that, during the formation of the protein complex with hemoglobin, the A_{41-56}, A_{69-90}, and $A_{128-139}$ fragments

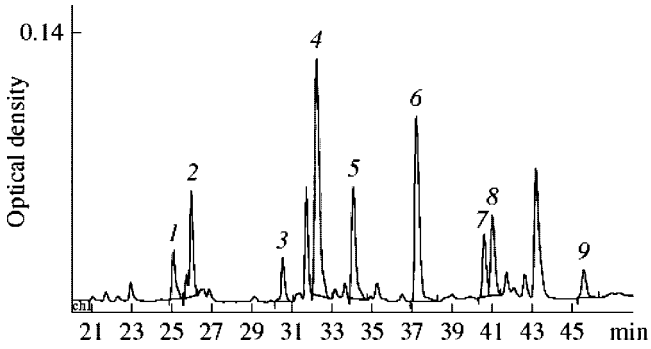

Figure 23. HPLC of peptides obtained by trypsin digestion of the tritium-labeled α-subunit of bovine hemoglobin on a column (150 mm × 3.9 mm) Delta Pac C8 in a gradient of concentration of a mixture of equal acetonitrile and methanol volumes (2−56%) in 0.1% TFA with the flow rate 1 mL/min: *1*, A_{93-99}; *2*, A_{17-31}; *3*, A_{91-99}; *4*, A_{41-56}; *5*, $A_{128-139}$; *6*, A_{32-40}; *7*, A_{69-90}; *8*, A_{69-92}; *9*, $A_{100-127}$. UV detection at 210 nm. Redrawn from ref 122.

retained their substitution ability of tritium for hydrogen, whereas that of A_{32-40} and A_{93-99} decreased by almost an order of magnitude. In the HSCIE reaction with a free α-subunit, the molar radioactivity of the isolated peptide MFLSFPTTK (A_{32-40}) was 15 Ci/mol, whereas for hemoglobin it was only 1.4 Ci/mol.

The changes in the peptide fragment reactivity toward SH, which originate from the spatial interactions of the subunits during protein complex formation, were evaluated by comparing these reactivity changes with any corresponding changes in their accessibility. The accessibility of the amino acids in the protein to the solution molecules has been recognized as the ratio of the amino acids surfaces in the protein to the amino acid free forms. Intermolecular interactions lead to a decrease in the accessibility of the fragments involved in these interactions. To describe the additional three-dimensional interactions between polypeptide chains, which take place in complex formation, the respective changes in the accessibility of the polypeptide amino acids to water (1.4 Å) were determined. In all cases, the evaluation was conducted for the 1.4 Å standard size of the water molecule. The calculation of the accessibility of the amino acids in hemoglobin was based on crystallographic data.[123]

It was shown that, in the formation of the hemoglobin−protein complex the three-dimensional interactions between the adjacent polypeptide chains resulted in decreased accessibility of the participating amino acid residues. The largest contribution to the three-dimensional interactions of the α_1-subunit is made by the β_1-subunit; the contribution of the β_2-subunit is only about half, and the interaction of the α_2-subunit is very small. The peptides of the α_1-subunit, whose reactivity changes considerably during complex formation, were shown to consist of amino acids whose accessibility, in this case, undergoes strong changes. The maximum change in reactivity was observed for the MELSFPTTK (A_{32-40}) peptide. Data presented in Table 19 show that this fragment interacts not only with the β_1 subunit but also with the β_2-subunit. The peptide fragments TYFPHFDLSHGSAQVK (A_{41-56}), AVEHLDDLPGALSELSDLHAHK (A_{69-90}), and FLANVSTVLTSK ($A_{128-129}$) predominantly contain those amino acids that do not change their accessibility during complex formation.

The method of accessibility calculation allows the accessibility of individual amino acid residues within a polypeptide to be evaluated. To estimate the accessibility of polypeptide fragments, the arithmetic mean of the water (1.4 Å) accessibility of the amino acid residues was used. Data in Table 20 shows the interconnection between the accessibility (1.4 Å) change of the peptide fragments and the change in their reactivity during complex formation.

These observations demonstrate that the peptide fragments Thr41-Lys56, Ala69-Lys90, Ala69-Arg92, and Phe128-Lys139 took a minor part in the protein complex formation. In this case, their accessibility for water decreases by no more than 2% and their reactivity toward SH is virtually unchanged. Meanwhile, the peptide fragments Met32-Lys40 and Val193-Lys99 played a considerable part in the interaction between the subunits (Figure 24). Their ability to

Table 20. Ratio of the Specific Radioactivity of the α_1-Subunit Tryptic Peptides Obtained from the HSCIE Reaction with Hemoglobin or with the Free α_1-Subunit, Depending on the Availability (1.4 Å) of the Corresponding Fragments within the Hemoglobin (I) Structure and in the Free α_1-Subunit (II)[a]

peptide	ratio of the specific radioactivity,[b] %	availability[c] (1.4 Å) of peptide fragments of the α chain, %	
		I	II
Val17−Arg31	0.51	28	32
Met32−Lys40	0.09	26	43
Thr41−Lys56	1.0	46	48
Ala69−Lys90	1.0	32	32
Ala69−Arg92	1.0	32	34
Leu91−Lys99	0.17	25	46
Val93−Lys99	0.10	23	43
Leu100−Lys127	0.41	21	32
Phe128−Lys139	0.92	27	29

[a] Redrawn from ref 122. [b] The specific radioactivity is a ratio of the peptide radioactivity in nCi to the area corresponding to its chromatographic peak using UV detection at 210 nm. [c] Availability for H_2O on the average per one amino acid residue of a peptide fragment.

Table 19. Specific Radioactivities of Tryptic Fragments of the Hemoglobin α-Subunit Obtained after HSCIE Reaction with the α-Subunit in the Free Form (I) or as the Protein Complex (II)[a]

peptide	amino acid sequence	M, Da	specific radioactivity[b], rel units	
			I	II
A_{17-31}	VGGHAAEYGAEALER	1528.73	2.4	1.22
A_{32-40}	MFLSFPTTK	1070.55	0.78	0.07
A_{41-56}	TYFPHFDLSHGSAQVK	1832.88	1.28	1.28
A_{69-90}	AVEHLDDLPGALSELSDLHAHK	2366.19	2.04	2.04
A_{69-92}	AVEHLDDLPGALSELSDLHAHKLR	2635.37	2.26	2.26
A_{91-99}	LRVDPVNFK	1086.62	3.3	0.56
A_{93-99}	VDPVNFK	817.43	3.0	0.30
$A_{100-127}$	LLSHSLLVTLASHLPSDFTPAVHASLDK	2968.60	3.52	1.44
$A_{128-139}$	FLANVSTVLTSK	1278.72	3.26	3.00

[a] Redrawn from ref 122. [b] The specific radioactivity is a ratio of the peptide radioactivity in nCi to the area of the corresponding chromatographic peak using UV detection at 210 nm.

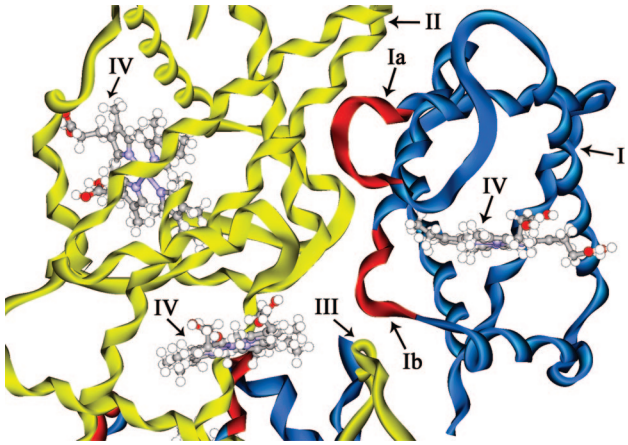

Figure 24. Spatial structure of bovine hemoglobin: I, α_1-subunit; Ia, fragment of α_1-subunit Met32-Lys40; Ib, fragment of α_1-subunit Val93-Lys99; II, β_1-subunit; III, β_2-subunit; IV, hemes. Redrawn from ref 122.

undergo solid state hydrogen exchange during complex formation falls by an order of magnitude with a 2-fold decrease in water accessibility. The reactivity of the peptide fragments Val17-Arg31 and Leu100-Lys127 during complex formation decreases by approximately two with a concomitant decrease in accessibility of 4−11%.

The observed dependences in isotope exchange in a protein complex can be interpreted in terms of contemporary concepts regarding the HSCIE reaction mechanism. It was earlier shown that hydrogen isotope exchange proceeds in the solid phase on the catalytic acidic centers formed under the action of SH.[74] The water of crystallization existing in the solid phase around the protein can play the role of proton acceptor. The water-inaccessible fragments of the protein molecule appear to be incapable of SH-affected isotope exchange. Information about isotope label incorporation into the individual amino acids during the protein complex HSCIE reaction permits the evaluation of the water cluster size in the Brønsted acidic centers involved in the reaction.

From the data presented it can be concluded that a comparison of the reactivities of the relevant regions of the protein complex polymer chain and the corresponding model-peptides makes it possible to identify the fragments of low accessibility within the complex. The low accessibility of the hemoglobin molecules for water leads to a decrease in reactivity, which results in considerable differences in the reactivity of the hemoglobin peptide fragments and the corresponding free peptides.

Analyzing the data obtained for the solid state isotope exchange in hemoglobin and in the α_1-subunit, we can conclude that the observed decrease of the hydrogen to spillover-tritium exchange ability in complex formation is related to the reduction in accessibility of the fragments participating in the interaction of the subunits. For the relatively large protein globule, the small contact areas appearing during the complex formation may be determined using the HSCIE reaction.

5. Conclusions

High temperature solid state catalytic isotope exchange (HSCIE) reactions take place in organic compounds under the action of spillover hydrogen (SH). The HSCIE reaction makes it possible to undertake an almost complete substitution of deuterium or tritium for hydrogen in a range of organic compounds while retaining the configuration of the asymmetric carbon atoms. To date the HSCIE reaction remains the only experimental opportunity for the synthesis of such uniformly labeled tritium compounds.

Isotopic equilibrium of the gaseous deuterium and hydrogen atoms of the solid organic compound has been established for HSCIE reactions. In these, the H−C substitution degree in the organic compound is determined only by the total ratio of isotope atoms in the reaction.

Highly tritium-labeled peptides containing the isotope label in all the amino acids which completely retain their enzymatic activity can be produced using HSCIE reactions. A considerable decrease in the ability to exchange hydrogen for SH in the contact area of the protein subunits has been demonstrated, and this can be used for identification of the contact area during complex formation in the proteins.

The HSCIE reaction takes place on Brønsted-type acidic centers formed under the action of SH according to the synchronous one-center mechanism. The transition state of this reaction is characterized by the formation of a penta-coordinated carbon and a three-center bond between the carbon and the incoming and outgoing hydrogen atoms. Isotopic effects observed in the UV absorption and fluorescence electronic spectra as well as theoretical studies on tritium- and deuterium-labeled organic compounds have been discussed in depth.

6. Abbreviations

BAC	Brønsted acidic centers
CtxG1	α-conotoxin G1
DALG	dalargine (Tyr-*D*-Ala-Gly-Phe-Leu-Arg)
HF	Hartree−Fock *ab initio* calculations
HSCIE	high temperature solid state catalytic isotope exchange
LENK	[Leu^5]-enkephalin (Tyr-Gly-Gly-Phe-Leu)
MAC	model acidic centers
MP2	Møller−Plesset perturbation theory
MS	mass spectrometry I
SH	spillover hydrogen
ZPC	zero-point energy corrections

7. References

(1) Conner, W. C.; Falconer, J. L. *Chem. Rev.* **1995**, *95*, 759.
(2) Khoobiar, S. J. *J. Phys. Chem.* **1964**, *68*, 411.
(3) Lamartine, R.; Perrin, R. In *Spillover of Absorbed Species*; Pajonk, G. M., Teichner, S. J., Germain, J. E. Ž., Eds.; Elsevier: Amsterdam, 1983; p 251.
(4) Levy, R. B.; Boudart, M. *J. Catal.* **1974**, *32*, 30.
(5) Braunschveig, Th.; Roland, U.; Winkler, H. *Stud. Surf. Sci. Catal.* **1993**, *17*, 53.
(6) Sotoni, N.; Eda, K.; Kunitomo, M. *J. Chem. Soc., Faraday Trans.* **1990**, *86*, 1583.
(7) Teichner, S. J. *Appl. Catal.* **1990**, *62*, 1.
(8) Corma, A. *Chem. Rev.* **1995**, *95*, 559.
(9) Yang, M.; Nakamura, I.; Fujuimoto, K. *J. Appl. Catal. Gen.* **1996**, *144*, 221.
(10) Stumbo, A. M.; Grande, P.; Delmon, B. *Stud. Surf. Sci. Catal.* **1997**, *12*, 211.
(11) Roessner, F.; Roland, U.; Braunschweig, T. *J. Chem. Soc., Faraday Trans.* **1995**, *91*, 1536.
(12) Fujimoto, K.; Tomishige, K.; Okabe, A. *J. Appl. Catal. Gen.* **2000**, *194−195*, 383.
(13) Kusakari, T.; Tomishige, K.; Fujimoto, K. *J. Appl. Catal. Gen.* **2002**, *224*, 219.
(14) Liu, Ya.; Koyano, G.; Misono, M. *Top. Catal.* **2000**, *11/12*, 239.
(15) Aimoto, K.; Fujimoto, K.; Maeda, K. *Stud. Surf. Sci. Catal.* **1993**, *77*, 165.
(16) Kikuchi, E.; Matsuda, T. *Stud. Surf. Sci. Catal.* **1993**, *77*, 53.
(17) Ebitani, K.; Tsuji, J.; Hattori, H.; Kita, H. *J. Catal.* **1992**, *135*, 609.

(18) Tanaka, T.; Ehilani, K.; Hattori, H.; Yoshida, S. *Stud. Surf. Sci. Catal.* **1993**, *77*, 285.
(19) Stumbo, A. M.; Grange, P.; Delmon, B. *Stud. Surf. Sci. Catal.* **1996**, *101*, 97.
(20) Gutsze, A.; Roland, U.; Karger, H. G. *Stud. Surf. Sci. Catal.* **1997**, *112*, 417.
(21) Holmberg, M.; Lundström, I. J. *Appl. Surf. Sci.* **1996**, *93*, 67.
(22) Stoica, M.; Caldararu, M.; Capritza, A.; Ionescu, N. I. J. *React. Kinet. Catal. Lett.* **1996**, *57*, 81.
(23) Roland, U.; Braunschweig, T.; Roessner, F. *J. Mol. Catal. A: Chem.* **1997**, *127*, 61.
(24) Roessner, F.; Roland, U. *J. Mol. Catal. A: Chem.* **1996**, *112*, 401.
(25) Franke, M. E.; Simon, U.; Roessner, F.; Roland, U. *Appl. Catal. A: Gen.* **2000**, *202*, 179.
(26) Roland, U.; Winkler, H.; Bauch, H.; Steinberg, K.-H. *J. Chem. Soc., Faraday Trans.* **1991**, *87*, 3921.
(27) Yaroslavtsev, A. B. *Usp. Khim.* **1994**, *63*, 449.
(28) Stumbo, A. M.; Grande, P.; Delmon, B. *Stud. Surf. Sci. Catal.* **1997**, *112*, 211.
(29) Willey, R. J.; Teichner, S. J.; Pajonk, G. M. *J. Mol. Catal.* **1992**, *77*, 201.
(30) Kosheleva, L. S. *Russ. Chem. Bull.* **1995**, *44*, 236.
(31) Roland, U.; Salzer, R.; Stolle, S. *Stud. Surf. Sci. Catal.* **1994**, *84*, 1231.
(32) Lomot, D.; Karpinski, Z. *Catal. Lett.* **2000**, *69*, 133.
(33) Pang, Y.-W.; Dalmond, B. J. *Mol. Catal.* **2001**, *169*, 259.
(34) Zolotarev, Yu. A.; Kozik, V. S.; Zaitsev, D. A.; Dorokhova, E. M.; Myasoedov, N. F. *Dokl. Chem.* **1989**, *308*, 1146.
(35) Zolotarev, Yu. A.; Kozic, V. S.; Zaitsev, D. A.; Dorokhova, E. M.; Myasoedov, N. F. *J. Radioanal. Nucl. Chem. Art.* **1992**, *162*, 3.
(36) Zolotarev, Yu. A.; Tatur, V. Yu.; Zaitsev, D. A.; Myasoedov, N. F. U.S. Patent 5026909, 1988.
(37) Zolotarev, Yu. A.; Zaitsev, D. A.; Myasoedov, N. F. *USSR Inventor's Certificate* No. 4 306 114, 1988.
(38) Zolotarev, Yu. A.; Kozik, V. S.; Dorokhova, E. M.; Zaitsev, D. A.; Rosenberg, S. G.; Myasoedov, N. F. In *Proceedings of the Fours International Symposium "Synthesis and Application of Isotopically Labelled Compounds*; Baillie, T. A., Jones, J. R., Eds.; Elsevier: 1992; p 687.
(39) Zolotarev, Yu. A.; Myasoedov, N. F.; Zaitsev, D. A.; Lubnin, M. Yu.; Tatur, V. Yu.; Kozik, V. S.; Dorochova, E. M.; Rozenberg, S. G. *Radioisotopes* **1990**, *31*, 110.
(40) Zolotarev, Yu. A.; Davankov, V. A. *J. Chromatogr.* **1978**, *155*, 285.
(41) Zolotarev, Yu. A.; Myasoedov, N. F.; Penkina, V. I.; Petrenik, O. V.; Davankov, V. A. *J. Chromatogr.* **1981**, *207*, 231.
(42) Zolotarev, Yu. A.; Zaitsev, D. A.; Dorochova, E. M.; Myasoedov, N. F. *J. Radioanal. Nucl. Chem., Art.* **1988**, *121*, 469.
(43) Zolotarev, Yu. A.; Kozik, V. S.; Zaitsev, D. A.; Dorochova, E. M.; Myasoedov, N. F. *J. Label. Compd.* **1991**, *29*, 507.
(44) Zolotarev, Yu. A.; Laskatelev, E. V.; Rosenberg, S. G.; Borisov, Yu. A.; Myasoedov, N. F. *Russ. Chem. Bull.* **1997**, *47*, 1536.
(45) Zolotarev, Yu. A.; Dadayan, A. K.; Borisov, Yu. A. *Russ. J. Bioorg. Chem.* **2005**, *31*, 1.
(46) Rozenberg, S. G.; Zaloznikh, V. M.; Zolotarev, Yu. A.; Kozic, V. S.; Myasoedov, N. F. *J. Radioanal. Nucl. Chem. Lett.* **1991**, *149*, 247.
(47) Zolotarev, Yu. A.; Kozik, V. S.; Dorochova, E. M.; Myasoedov, N. F. *J. Label. Compd.* **1992**, *31*, 71.
(48) Zolotarev, Yu. A.; Dorokhova, E. M.; Nezavibatko, V. N.; Borisov, Yu. A.; Rosenberg, S. G.; Velikodvorskaia, G. A.; Neumivakin, L. V.; Zverlov, V. V.; Myasoedov, N. F. *Amino Acids* **1995**, *8*, 353.
(49) Rosenberg, S. G.; Zolotarev, Yu. A.; Myasoedov, N. F. *Amino Acids* **1991**, *3*, 95.
(50) Zolotarev, Yu. A.; Laskatelev, E. V.; Dorokhova, E. M.; Borisov, Yu. A.; Rosenberg, S. G.; Myasoedov, N. F. *Russ. Chem. Bull.* **1997**, *46*, 726–731.
(51) Zolotarev, Yu. A.; Laskatelev, E. V.; Dorokhova, E. M.; Borisov, Yu. A.; Rosenberg, S. G.; Myasoedov, N. F. *Proceedings of the Fifth International Symposium on Synthesis and Application of Isotopically Labelled Compounds*; Allen, J., Voges, R., Eds.; Elsevier: 1995; p 185.
(52) Kozik, V. S.; Zolotarev, Yu. A.; Dorochova, E. M.; Myasoedov, N. F. *Proceedings of the Third International Symposium on Synthesis and Application of Isotopically Labelled Compounds*; Baillie, T. A., Jones, J. R., Eds.; Elsevier: 1989; p 513.
(53) Zolotarev, Yu. A.; Kozik, V. S.; Dorokhova, E. M.; Myasoedov, N. F. *Proceedings of the Fourth International Symposium on Synthesis and Application of Isotopically Labelled Compounds*; Baillie, T. A., Jones, J. R., Eds.; Elsevier: 1992; p 498.
(54) Zolotarev, Yu. A.; Kozic, V. S.; Dorochova, E. M.; Myasoedov, N. F. *J. Labelled Compd.* **1991**, *29*, 997.
(55) Zolotarev, Yu. A.; Laskatelev, E. V.; Kozik, V. S.; Dorokhova, E. M.; Rosenberg, S. G.; Borisov, Yu. A.; Myasoedov, N. F. *Russ. Chem. Bull.* **1997**, *46*, 1726.
(56) Eller, M.; Zaitsev, D.; Fransson, B.; Jarv, J.; Myasoedov, N.; Ragnarsson, U. *Bioorg. Chem.* **1992**, *20*, 245.
(57) Zolotarev, Yu. A.; Firsova, Yu. Yu.; Abaimov, D. A.; Dadayan, A. K.; Kosik, V. S.; Novikov, A. V.; Krasnov, N. V.; Vaskovskii, B. V.; Nazimov, I. V.; Kovalev, G. I.; Myasoedov, N. F. *Russ. J. Bioorg. Chem.* **2009**, *35*, 296.
(58) Zolotarev, Yu. A.; Dadayan, A. K.; Kozik, V. S.; Ziganshin, R. H.; Vaskovsky, B. V.; Myasoedov, N. F. *J. Label Compd. Radiopharm.* **2007**, *50*, 483.
(59) Wong, E. H. F.; Kemp, J. A.; Priestley, T.; Knight, A. R.; Woodruff, G. N.; Iversen, L. L. *Proc. Natl. Acad. Sci. U.S.A.* **1986**, *83*, 7104.
(60) Shishkov, A. V.; Filatov, E. S.; Simonov, E. F.; Unukovich, M. S.; Gol'danskii, V. I.; Nesmeyanov, A. N. *Dokl. Akad. Nauk SSSR* **1976**, *228*, 1237.
(61) Shishkov, A. V.; Baratova, L. A. *Usp. Khim.* **1994**, *63*, 825.
(62) Agafonov, D. E.; Kolb, V. A.; Spirin, A. S. *Proc. Natl. Acad. Sci. U.S.A.* **1997**, *94*, 12892.
(63) Shishkov, A. V.; Goldanskii, V. I.; Baratova, L. A.; Fedorova, N. V.; Ksenofontov, A. L.; Zhirnov, O. P.; Galkin, A. V. *Proc. Natl. Acad. Sci. USA* **1999**, *96*, 7827.
(64) Simonov, E. F.; Unukovich, M. S.; Filatov, E. S.; Shishkov, A. V. *Khim. Vys. Energ.* **1978**, *12*, 8.
(65) Baratova, L. A.; Rumyantsev, Yu. M.; Simonov, E. F.; Unukovich, M. S.; Tsyryapkin, V. A.; Shishkov, A. V. *Khim. Vys. Energ.* **1981**, *15*, 370.
(66) Orlova, M. A.; Nesmeyanov, A. N. *Radiochemistry* **1981**, *20*, 787.
(67) Kolodziejzyk, K.; Arendt, A. *Roczn. Chem.* **1977**, *51*, 659.
(68) Evans, E. A.; Sheppard, H. C.; Turner, J. C.; Warrell, D. C. J. *Label. Compd.* **1974**, *10*, 569.
(69) Borisov, Yu. A.; Zolotarev, Yu. A.; Laskatelev, E. V.; Myasoedov, N. F. *Russ. Chem. Bull* **1997**, *46*, 407.
(70) Fleisch, T.; Aberman, R. *J. Catal.* **1977**, *50*, 268.
(71) Keren, E.; Soffer, A. *J. Catal.* **1977**, *50*, 43.
(72) Rozanov, V. V.; Krilov, O. V. *Russ. Chem. Rev.* **1997**, *66*, 117.
(73) Yamabe, S.; Osamura, Y.; Minato, T. J. *Am. Chem. Soc.* **1980**, *102*, 2268.
(74) Borisov, Yu. A.; Zolotarev, Yu. A.; Laskatelev, E. V.; Myasoedov, N. F. *Russ. Chem. Bull* **1996**, *45*, 1754.
(75) Borisov, Yu. A.; Zolotarev, Yu. A. *Russ. Chem. Bull.* **1999**, *48*, 1431.
(76) Borisov, Yu. A.; Zolotarev, Yu. A.; Laskatelev, E. V.; Myasoedov, N. F. *Russ. Chem. Bull.* **1998**, *47*, 1442.
(77) Evleth, E. M.; Kassab, E.; Sierra, L. R. *J. Phys. Chem.* **1994**, *98*, 1421.
(78) Zolotarev, Yu. A.; Borisov, Yu. A.; Myasoedov, N. F. *J. Phys. Chem.* **1999**, *103*, 4861.
(79) Woon, D. E.; Dunning, T. H. *J. Chem. Phys.* **1993**, *98*, 1358.
(80) Borisov, Yu. A.; Zolotarev, Yu. A. *Rus. J. Phys. Chem.* **2002**, *76*, 635.
(81) Szulejko, J. E.; McMahon, T. B. *J. Am. Chem. Soc.* **1993**, *115*, 7839.
(82) Brown, G. M.; Noe-Spirlet, M. R.; Busing, W. R.; Levy, H. A. *Acta Crystallogr., Sect B: Struct. Sci.* **1977**, *33*, 1038.
(83) Krossner, M.; Sauer, J. *J. Phys. Chem.* **1996**, *100*, 6199.
(84) Jentys, A.; Warecka, G.; Derewinski, M.; Lercher, J. A. *J. Phys. Chem.* **1989**, *93*, 4837.
(85) Marchese, L.; Chen, J.; Wright, P. A.; Thomas, J. M. *J. Phys. Chem.* **1993**, *97*, 8109.
(86) Pelmenschikov, A. G.; van Santen, R. A. *J. Phys. Chem.* **1993**, *97*, 10678.
(87) Nusterer, E.; Blochl, P. E.; Schwartz, K. *Chem. Phys. Lett.* **1996**, *253*, 448.
(88) Haw, J. F.; Xu, T.; Nicolas, J. B.; Gogguen, P. W. *Nature* **1997**, *389*, 832.
(89) Nicolas, J. B.; Haw, J. F. J. *Am. Chem. Soc.* **1998**, *120*, 11804.
(90) Xu, T.; Barich, D. H.; Goguen, P. W.; Song, W.; Wang, Z.; Nicolas, J. B.; Haw, J. F. *J. Am. Chem. Soc.* **1998**, *120*, 4025.
(91) Liu, X.; Iu, K.; Thomas, J. K.; He, H.; Klinowski, J. *J. Am. Chem. Soc.* **1994**, *116*, 11811.
(92) Beck, L. W.; Xu, T.; Nicolas, J. B. *J. Am. Chem. Soc.* **1995**, *117*, 11594.
(93) Yang, M.; Nakamura, I.; Fujuimoto, K. *J. Appl. Catal., Gen.* **1996**, *144*, 221.
(94) Nicholas, J. B.; Haw, J. F.; Beck, L. W.; Krawietz, T. R.; Ferguson, D. B. *J. Am. Chem. Soc.* **1995**, *117*, 12350.
(95) Zolotarev, Yu. A.; Borisov, Yu. A. *Russ. Chem. Bull.* **1999**, *48*, 1044.
(96) Zolotarev, Yu. A.; Borisov, Yu. A.; Myasoedov, N. F. In *Proceedings of the Sixth International Symposium on Synthesis and Application of Isotopically Labelled Compounds*; Heys, J. R., Melillo, D. G., Eds.; Wiley: New York, 1997; p 653.
(97) Rettig, W., Strehmel, B., Schrader, S., Seifert, H., Eds. *Applied Fluorescence in Chemistry, Biology and Medicine*; Springer: Berlin-Heidelberg, 1999.
(98) McLaughlin, M. L.; Barkley, M. D. *Methods Enzymol.* **1997**, *278*, 191.

(99) Zolotarev, Yu. A.; Dadayan, A. K.; Borisov, Yu. A.; Myasoedov, N. F. *Dokl. Phys. Chem.* **2005**, *400*, 15, Part 2.
(100) Zolotarev, Yu. A.; Dadayan, A. K.; Borisov, Yu. A.; Myasoedov, N. F. *THEOCHEM* **2005**, *724*, 53.
(101) Becke, A. D. *J. Chem. Phys.* **1993**, *98*, 5648.
(102) Foresman, J. B.; Head-Gordon, M.; Pople, J. A.; Frish, M. J. *J. Phys. Chem.* **1992**, *96*, 135.
(103) Zolotarev, Yu. A.; Dadayan, A. K.; Borisov, Yu. A.; Myasoedov, N. F. *Amino Acids* **2006**, *31*, 403.
(104) Zaitsev, D. A.; Zolotarev, Yu. A.; Myasoedov, N. F. *Dokl. Chem.* **1990**, *313*, 619.
(105) Klimova, O. A.; Zolotarev, Yu. A.; Chebotarev, V. Yu. *Biochem. Biophys. Res. Commun.* **1993**, *195*, 758.
(106) Kolobov, A. A.; Kolodkin, N. I.; Tuthill, C.; Zolotarev, Yu. A.; Navolotskaya, E. V. *Int. J. Pept. Res. Ther.* **2008**, *14*, 97.
(107) Zolotarev, Yu. A.; Dadayan, A. K.; Bocharov, E. V.; Borisov, Yu. A.; Vaskovsky, B. V.; Dorokhova, E. M.; Myasoedov, N. F. *Amino Acids* **2003**, *24*, 325.
(108) Zolotarev, Yu. A.; Dadayan, A. K.; Dolotov, O. V.; Kozik, V. S.; Kost, N. V.; Sokolov, O. Yu.; Dorokhova, E. M.; Meshavkin, V. K.; Inozemtseva, L. S.; Gabaeva, M. V.; Andreeva, L. A.; Alfeeva, L. Yu.; Pavlov, T. S.; Badmaeva, K. E.; Badmaeva, S. E.; Bakaeva, Z. V.; Kopylova, G. N.; Samonina, G. E.; Vaskovsky, B. V.; Grivennikov, I. A.; Zozulya, A. A.; Myasoedov, N. F. *Russ. J. Bioorg. Chem.* **2006**, *32*, 166.
(109) Navolotskaya, E. V.; Kovalitskaya, Yu. A.; Zolotarev, Yu. A.; Kudryashova, N. Yu.; Goncharenko, E. N.; Kolobov, A. A.; Kampe-Nemm, E. A.; Malkova, N. V.; Yurovsky, V. V.; Lipkin, V. M. *Peptides* **2003**, *24*, 1941.
(110) Navolotskaya, E. V.; Vanina, V. I.; Zolotarev, Yu. A.; Kudryashova, N. Yu.; Goncharenko, E. N.; Kolobov, A. A.; Kampe-Nemm, E. A.; Yurovsky, V. V.; Lipkin, V. M. *Regul. Pept.* **2004**, *119*, 99.
(111) Dolotov, O. V.; Inozemtseva, L. S.; Zolotarev, Yu. A.; Andreeva, L. A.; Alfeeva, L. Yu.; Grivennikov, I. A.; Myasoedov, N. F. *J. Neurochem.* **2006**, *97* (s1), 82.
(112) Grivennikov, I. A.; Dolotov, O. V.; Zolotarev, Yu. A.; Andreeva, L. A.; Myasoedov, N. F.; Licher, L.; Black, I. B.; Dreyfus, C. F. *Restor. Neurol. Neurosci.* **2008**, *26* (s1), 35.
(113) Zolotarev, Yu. A.; Dolotov, O. V.; Inozemtseva, L. S.; Dadayan, A. K.; Dorokhova, E. M.; Andreeva, L. A.; Alfeeva, L. Yu.; Grivennikov, I. A.; Myasoedov, N. F. *Amino Acids* **2006**, *30*, 403.
(114) Zolotarev, Yu. A.; Sokolov, O. Yu.; Kost, N. V.; Vaskovsky, B. V.; Myasoedov, N. F.; Zozulya, A. A. *Russ. J. Bioorg. Chem.* **2004**, *30*, 234.
(115) Dolotov, O. V.; Zolotarev, Yu. A.; Andreeva, L. A.; Grivennikov, I. A.; Myasoedov, N. F.; Russ, J. *Bioorg. Chem.* **2004**, *30*, 241.
(116) Zolotarev, Yu. A.; Dadayan, A. K.; Vaskovsky, B. V.; Kost, N. V.; Garanin, S. K.; Makarenkova, V. P.; Miasoedov, N. F. *Russ. J. Bioorg. Chem.* **2000**, *26*, 457.
(117) Navolotskaya, E. V.; Kovalitskaya, Y. A.; Sadovnikov, V. B.; Zolotarev, Yu. A.; Kolobov, A. A.; Yurovsky, V. V.; Lipkin, V. M. *Int. J. Pept. Res. Ther.* **2008**, *14*, 10.
(118) Koradi, R.; Billeter, M.; Wüthrich, K. *J. Mol. Graphics* **1996**, *14*, 51.
(119) Maslennikov, I. V.; Sobol, A. G.; Gladky, K. V.; Lugovskoy, A. A.; Ostrovsky, A. G.; Tsetlin, V. I.; Ivanov, V. T.; Arseniev, A. S. *Eur. J. Biochem.* **1998**, *254*, 238.
(120) Balashova, T. A.; Shenkarev, Z. O.; Tagaev, A. A.; Ovchinnikova, T. V.; Raap, J.; Arseniev, A. S. *FEBS Lett.* **2000**, *466*, 333.
(121) Zolotarev, Yu. A.; Dadayan, A. K.; Borisov, Yu. A.; Dorokhova, E. M.; Kozik, V. S.; Vtyurin, N. N.; Bocharov, E. V.; Ziganshin, R. N.; Lunina, N. A.; Kostrov, S. V.; Ovchinnikova, T. V.; Myasoedov, N. F. *Bioorg. Chem* **2003**, *31*, 453.
(122) Zolotarev, Yu. A.; Dadayan, A. K.; Ziganshin, R. Kh.; Borisov, Yu. A.; Kozik, V. S.; Dorokhova, E. M.; Vaskovsky, B. V.; Myasoedov, N. F. *Russ. J. Bioorg. Chem.* **2009**, *35*, 24.
(123) Mueser, T. C.; Rogers, P. H.; Arnone, A. *Biochemistry* **2000**, *39*, 15353.

CR100053W